Generalised continua in biomechanics : from multi scale tissues to biomechanical metamaterials

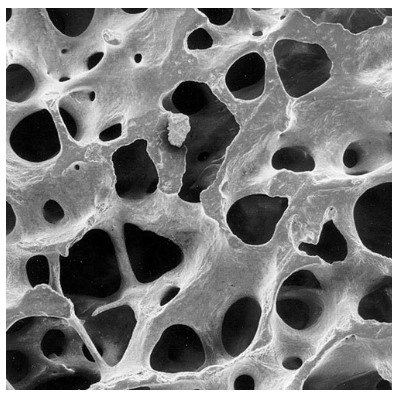

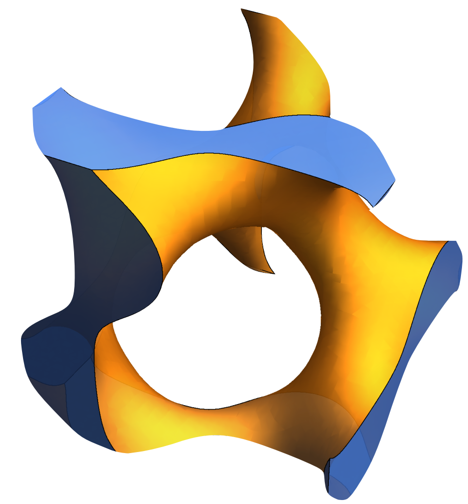

Giuseppe Rosi, Nicolas Auffray

Multi-Scale Modelling and Simulation Laboratory
Laboratoire Modélisation et Simulation Multi-Echelle
Université Paris-Est CNRS UMR 8208

ELADYN-BIO workshop
12-11-2020

Financed by: IRP Coss&Vita and ANR MAX-OASIS

PROJET FINANCÉ PAR L'ANR - PROJECT FUNDED BY THE ANR

Coss&Vita

MSME Laboratoire Modélisation et Simulation Multi Echelle

cnrs dépasser les frontières

UPEC UNIVERSITÉ PARIS-EST CRÉTEIL VAL DE MARNE Connaissance - Action

Context : elastic waves and ultrasounds

Elastic waves are currently used in several fields, such as non-destructive evaluation, characterisation, and diagnostics.

Principle : when a wave propagates inside a material, it carries information about the mechanical properties of the material itself.

Information is extracted solving an **inverse problem.**

Context : elastic waves and ultrasounds

Elastic waves are currently used in several fields, such as non-destructive evaluation, characterisation, and diagnostics.

Principle : when a wave propagates inside a material, it carries information about the mechanical properties of the material itself.

Information is extracted solving an **inverse problem.**

Main strategies:

Time of flight, amplitude

Bulk propagation and reflections at boundaries (imaging)

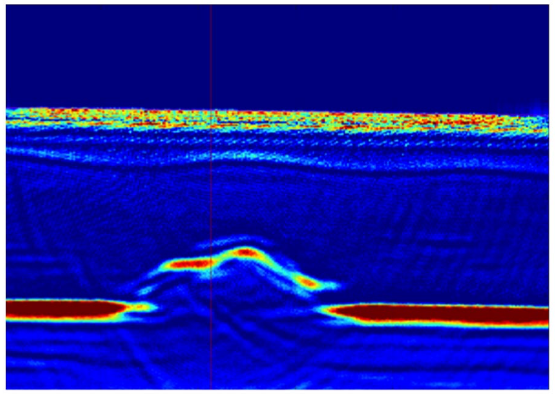

Dispersion

Guided propagation (surface waves, Lamb waves)

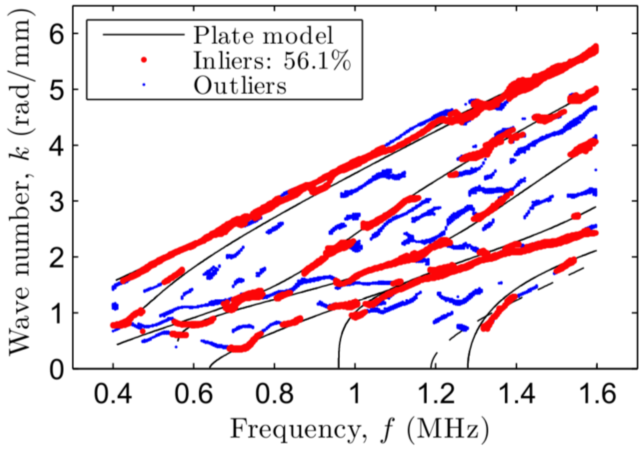

Bochud, N. et al (2017). Predicting bone strength with ultrasonic guided waves. Scientific Reports, 7, 43628

Multi scale tissue modelling and characterisation

Organ scale

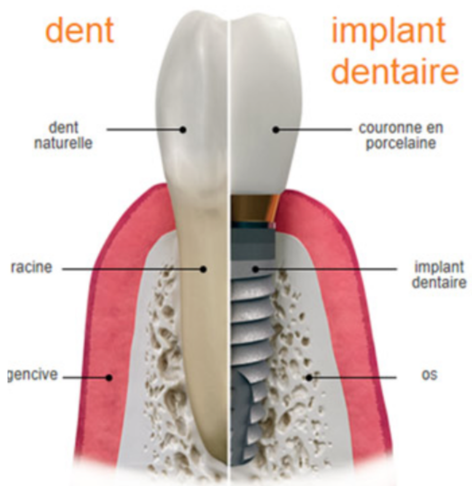

Dental implant

Orthopaedic implant


Bone scaffold implant

Multi scale tissue modelling and characterisation

Organ scale

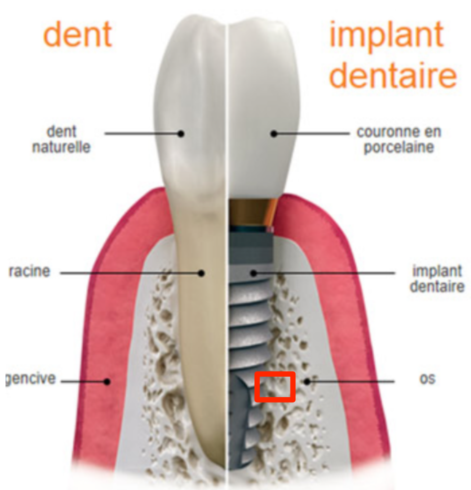

Dental implant

Orthopaedic implant

Bone scaffold implant

Tissue scale

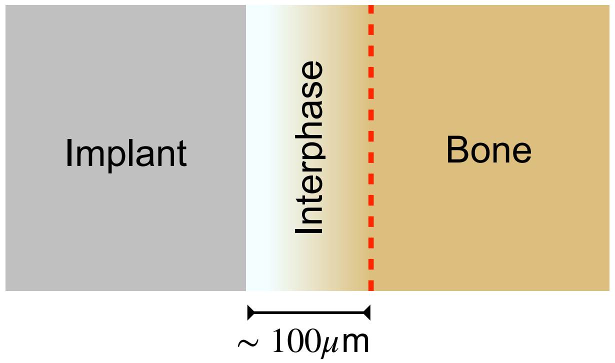

Multi scale tissue modelling and characterisation

Organ scale

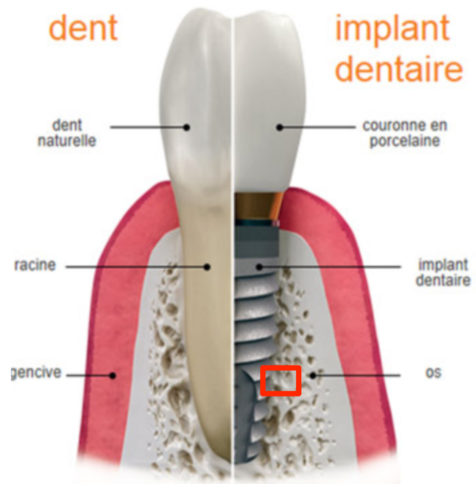

Dental implant

Orthopaedic implant

Bone scaffold implant

Tissue scale

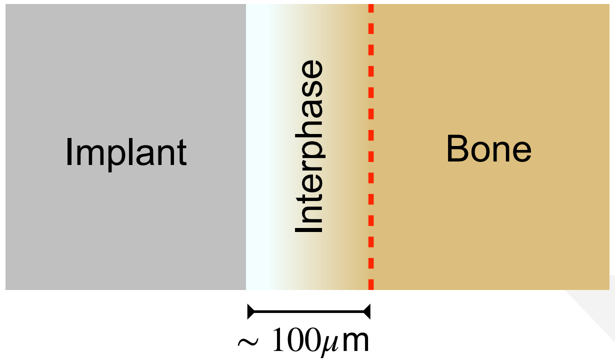

Architecture scale

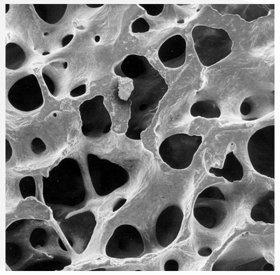

Bone

Multi scale tissue modelling and characterisation

Organ scale

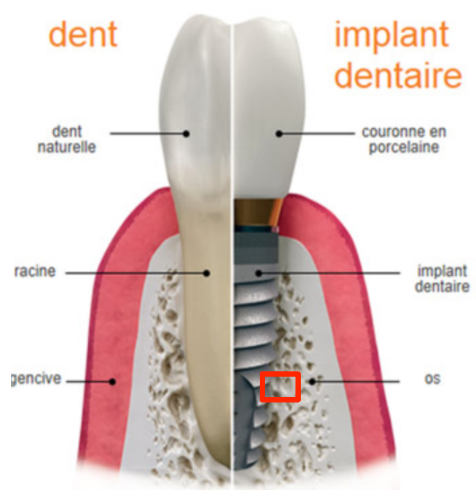

Dental implant

Orthopaedic implant

Bone scaffold implant

Tissue scale

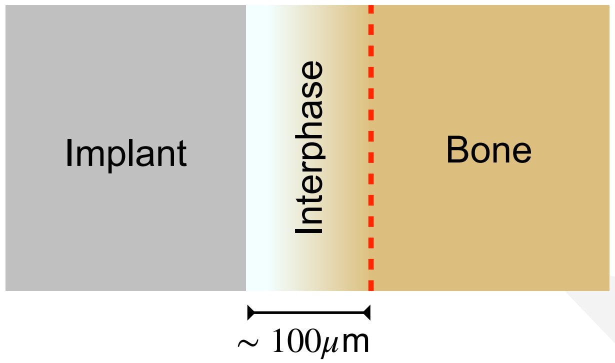

Architecture scale

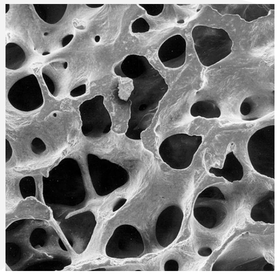

Bone

Modelling challenges

- Multi-scale architecture
- Heterogeneity
- Porosity
- Remodelling
- Boundary conditions

Multi scale tissue modelling and characterisation

Organ scale

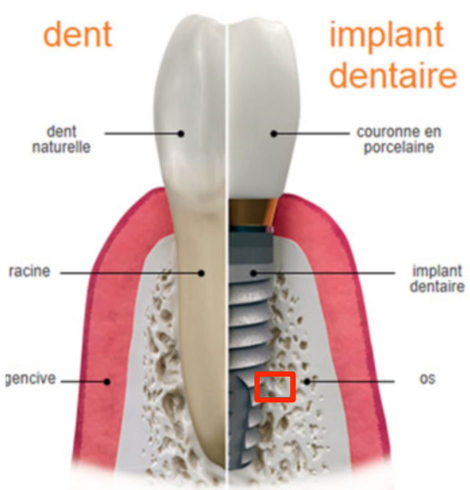

Dental implant

Orthopaedic implant

Bone scaffold implant

Tissue scale

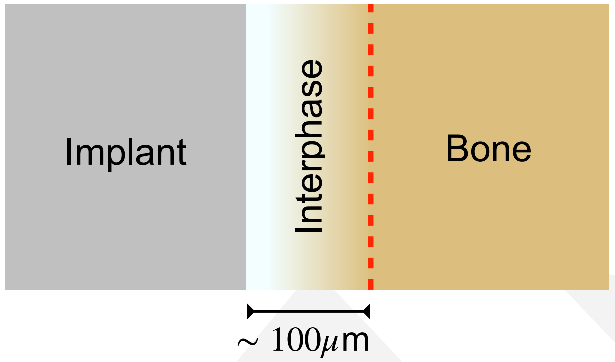

Architecture scale

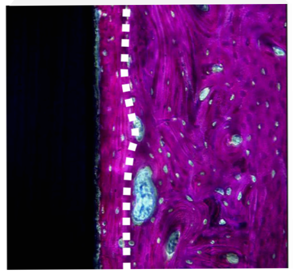

Interphase

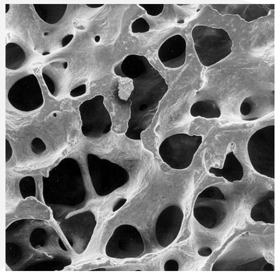

Bone

Modelling challenges

Interphase	Bone
Heterogeneity	Multi-scale architecture
Mesh refinement	Heterogeneity
Computational costs	Porosity
Evolving conditions (osteointegration)	Remodelling
Boundary conditions	Boundary conditions

Multi scale tissue modelling and characterisation

Organ scale

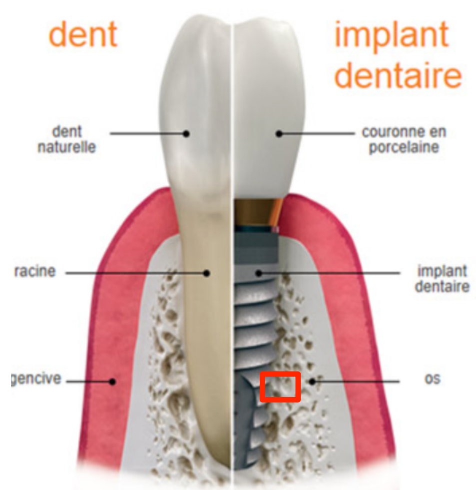

Dental implant

Orthopaedic implant

Bone scaffold implant

Tissue scale

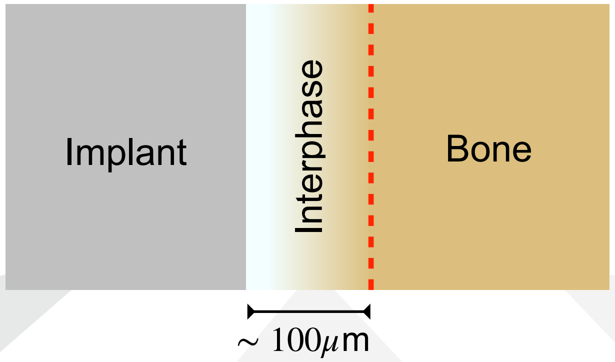

Architecture scale

Implant

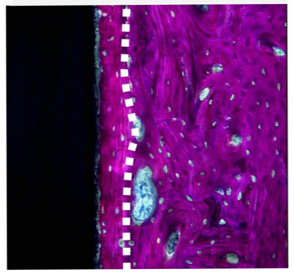

Interphase

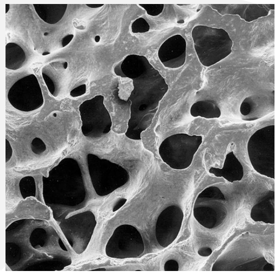

Bone

Modelling challenges

Interphase

Heterogeneity
Mesh refinement
Computational costs
Evolving conditions (osteointegration)
Boundary conditions

Bone

Multi-scale architecture
Heterogeneity
Porosity
Remodelling
Boundary conditions

Multi scale tissue modelling and characterisation

Organ scale

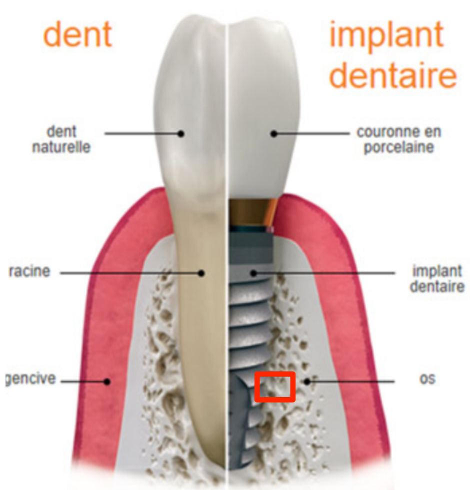

Dental implant

Orthopaedic implant


Bone scaffold implant

Tissue scale

Architecture scale

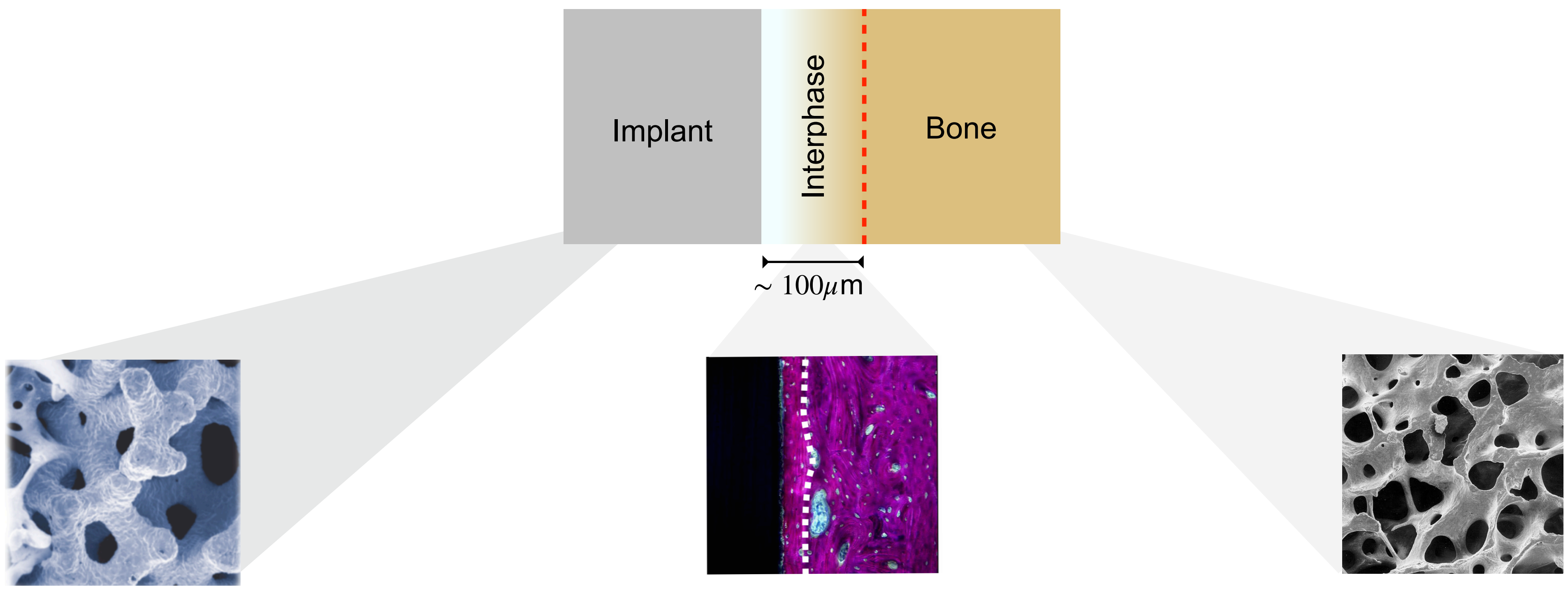

Implant

Interphase

Bone

Modelling challenges

Implant
- Multi-scale architecture
- Porosity
- Tissue engineering
- Multiple optimisation constraints
- Boundary conditions

Interphase
- Heterogeneity
- Mesh refinement
- Computational costs
- Evolving conditions (osteointegration)
- Boundary conditions

Bone
- Multi-scale architecture
- Heterogeneity
- Porosity
- Remodelling
- Boundary conditions

Multi scale tissue modelling and characterisation

Organ scale

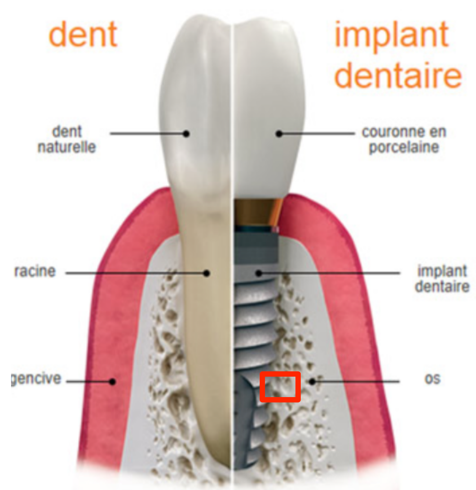

Dental implant

Orthopaedic implant

Bone scaffold implant

Tissue scale

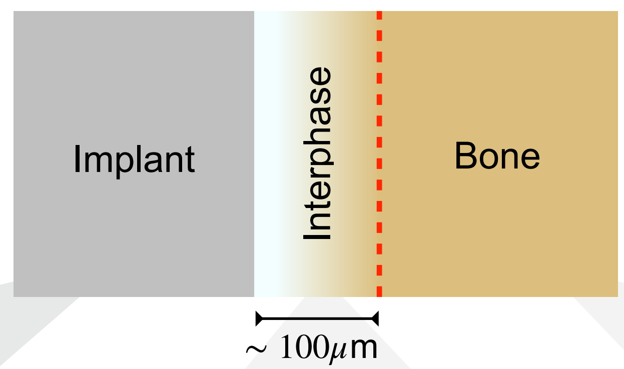

Architecture scale

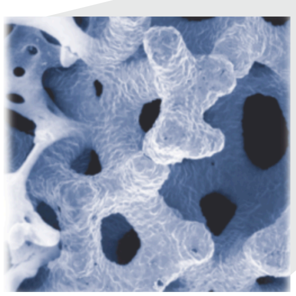

Implant

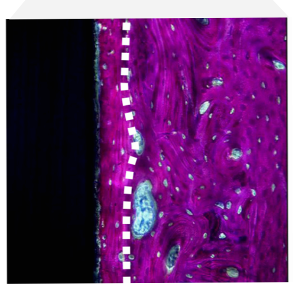

Interphase

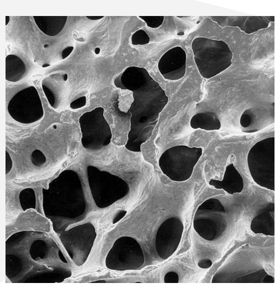

Bone

Modelling challenges

Implant
- Multi-scale architecture
- Porosity
- Tissue engineering
- Multiple optimisation constraints
- Boundary conditions

Interphase
- Heterogeneity
- Mesh refinement
- Computational costs
- Evolving conditions (osteointegration)
- Boundary conditions

Bone
- Multi-scale architecture
- Heterogeneity
- Porosity
- Remodelling
- Boundary conditions

Multi scale tissue modelling and characterisation

Organ scale

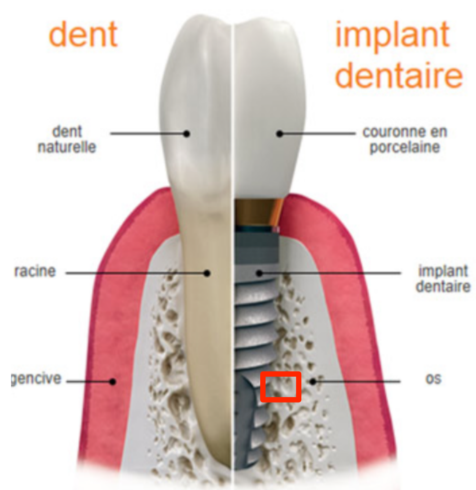

Dental implant

Orthopaedic implant

Bone scaffold implant

Tissue scale

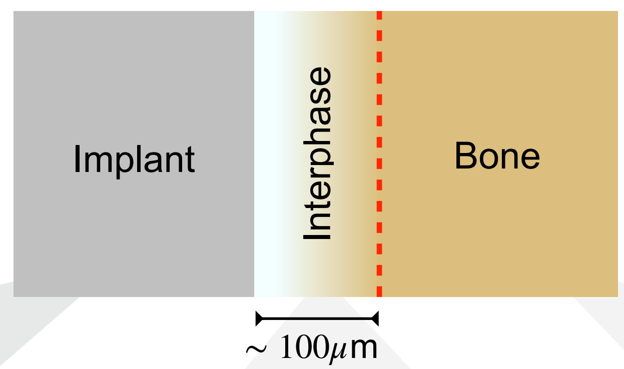

Architecture scale

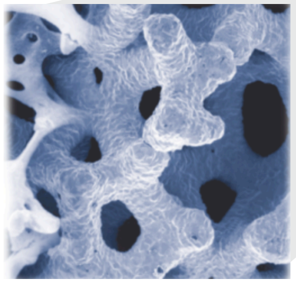

Implant

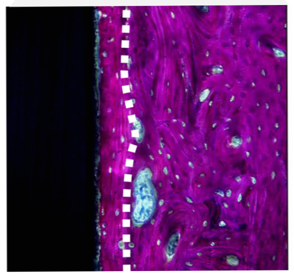

Interphase

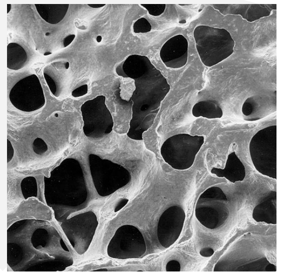

Bone

Modelling challenges

Implant
- Multi-scale architecture
- Porosity
- Tissue engineering
- Multiple optimisation constraints
- Boundary conditions

Interphase
- Heterogeneity
- Mesh refinement
- Computational costs
- Evolving conditions (osteointegration)
- Boundary conditions

Bone
- Multi-scale architecture
- Heterogeneity
- Porosity
- Remodelling
- Boundary conditions

Architectured implants as biomechanical metamaterials

Optimisation of the mechanical properties or reduction of stress shielding

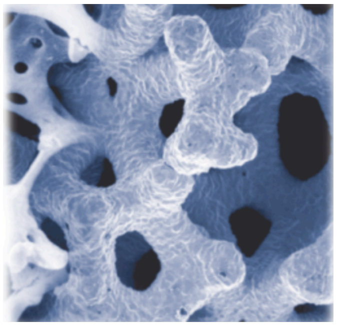

Zimmer's
Trabecular metal™
(Tantalum)

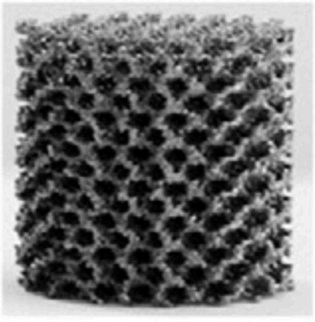

Gyroid scaffold
(Titanium)

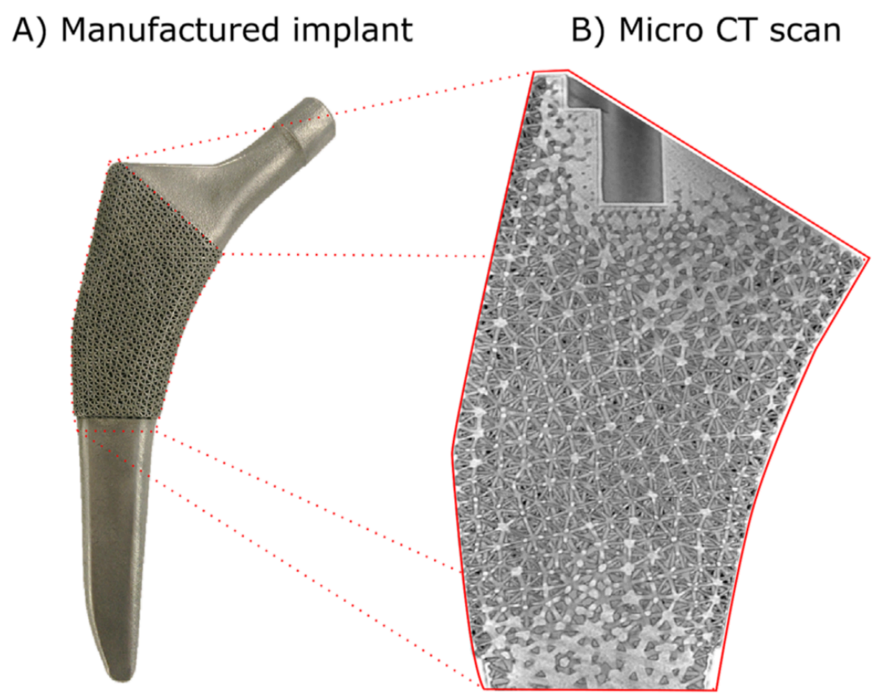

Fully porous implant
(Titanium)

Challenges and objectives:

- Take into account architecture and size effects in modelling
- Enhanced monitoring of the state of the implant
- Cost (or utility) functions to be used in optimisation

Results developed for metamaterials can be used

Yánez, A. et al. (2018). Gyroid porous titanium structures: A versatile solution to be used as scaffolds in bone defect reconstruction. Materials & Design, 140, 21–29.

Arabnejad, S. et al. (2017). Fully porous 3D printed titanium femoral stem to reduce stress-shielding following total hip arthroplasty. Journal of Orthopaedic Research, 35(8), 1774–1783.

Nature loves regular architectures!

Hexagonal honeycomb maximise the area vs the perimeter (for regular tilings) and isotropic mechanical properties

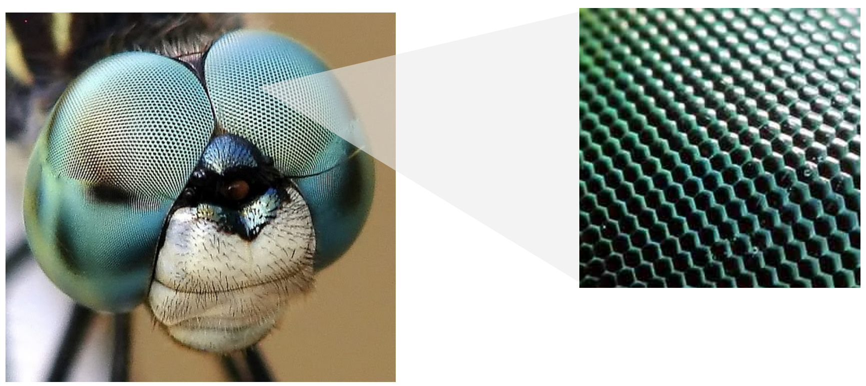

Gyroids are a minimal surfaces (obtained e.g. as assembly of co-block polymers) and are used as photonic crystals

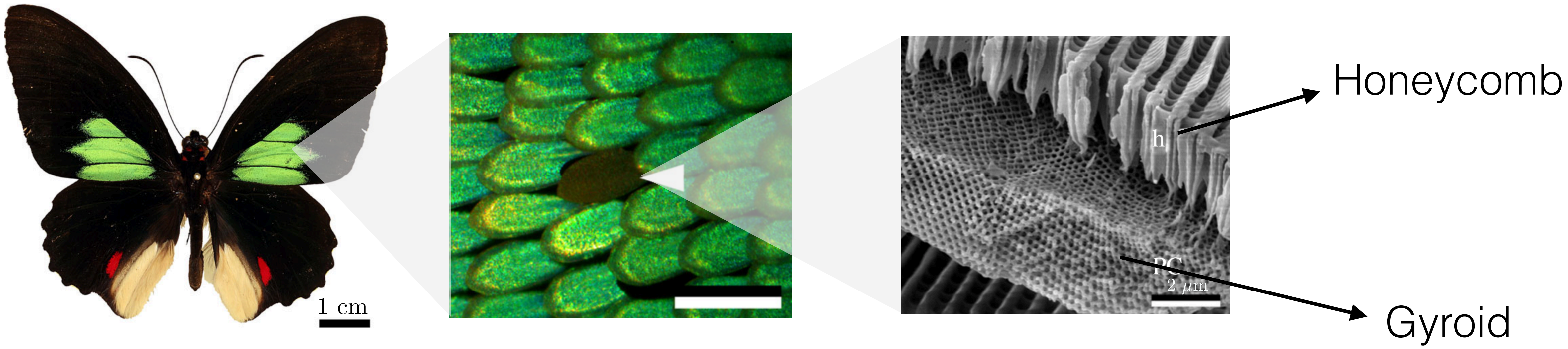

Hales, T. C. (2001). The Honeycomb Conjecture. Discrete & Computational Geometry, 25(1), 1–22.
Dolan et al. (2014). Optical Properties of Gyroid Structured Materials: From Photonic Crystals to Metamaterials. Advanced Optical Materials, 3(1), 12–32.
Wilts, B. D. et al (2012) Iridescence and spectral filtering of the gyroid-type photonic crystals in Parides sesostris wing scales. Interface Focus.

Wave propagation in hexagonal honeycombs

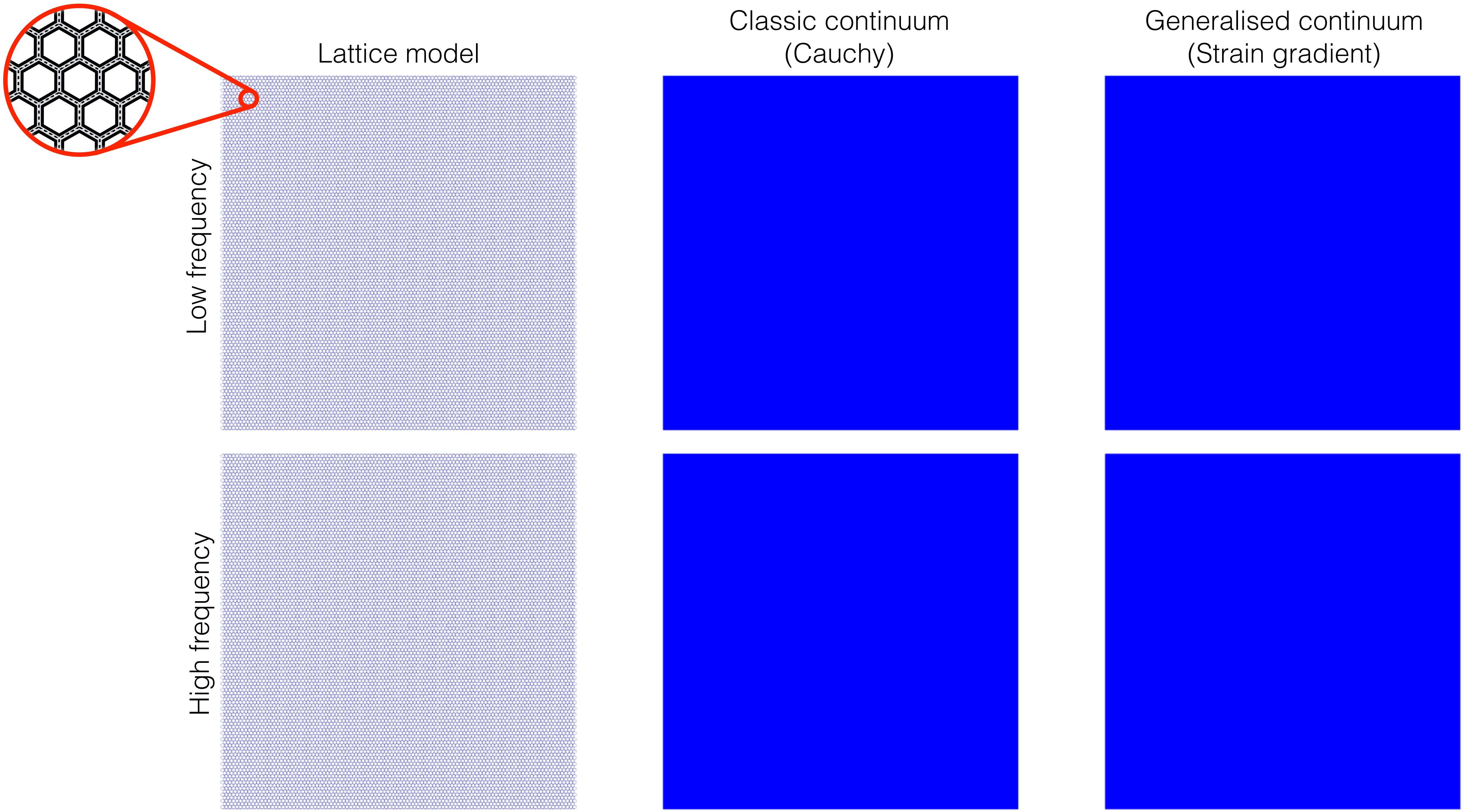

Wave propagation in architectured materials is not fully captured by a classic continuum

G. Rosi and N. Auffray, Continuum modelling of frequency dependent acoustic beam focusing and steering in hexagonal lattices, EJM/A

Wave propagation in hexagonal honeycombs

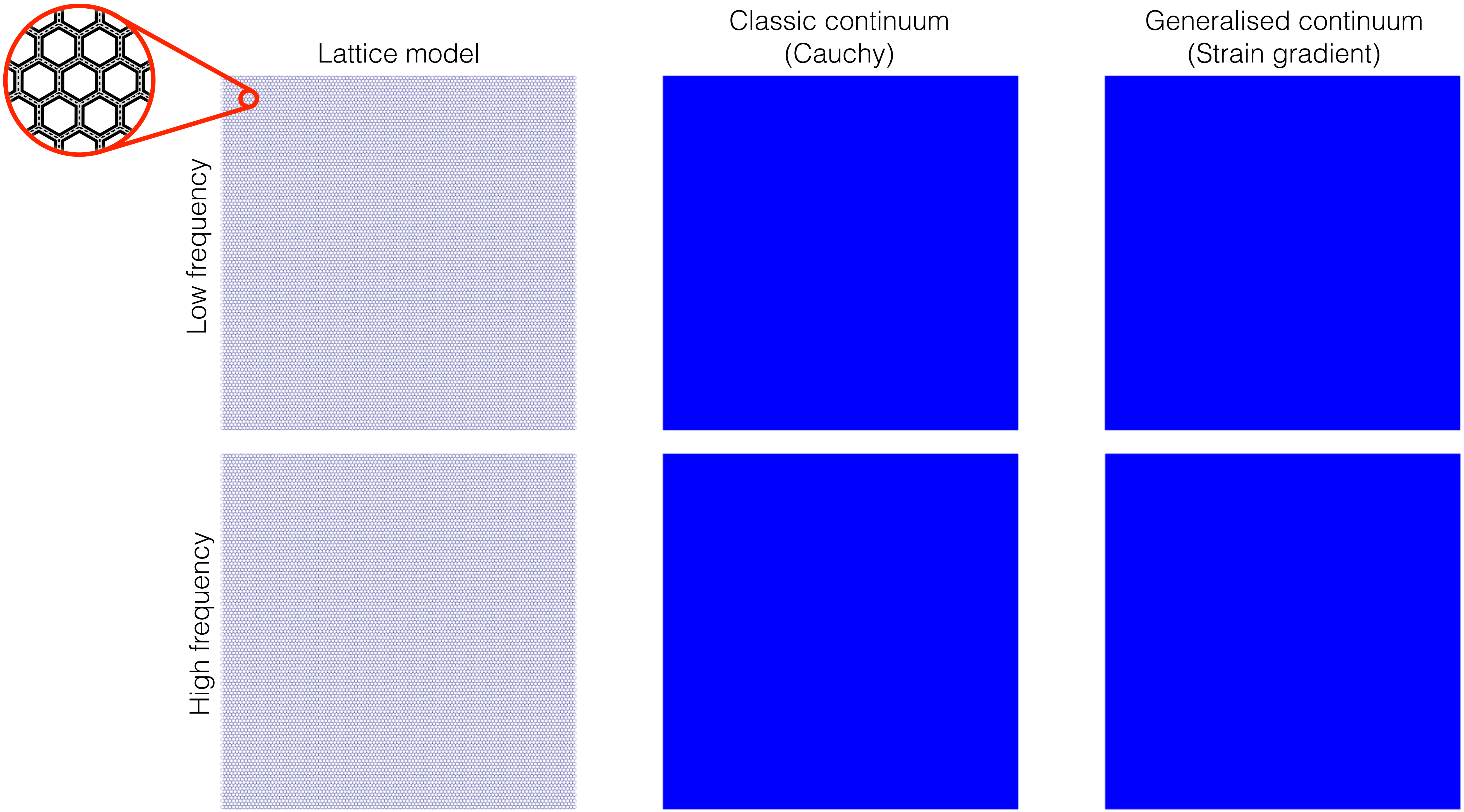

Wave propagation in architectured materials is not fully captured by a classic continuum

G. Rosi and N. Auffray, Continuum modelling of frequency dependent acoustic beam focusing and steering in hexagonal lattices, EJM/A

Wave propagation in hexagonal honeycombs

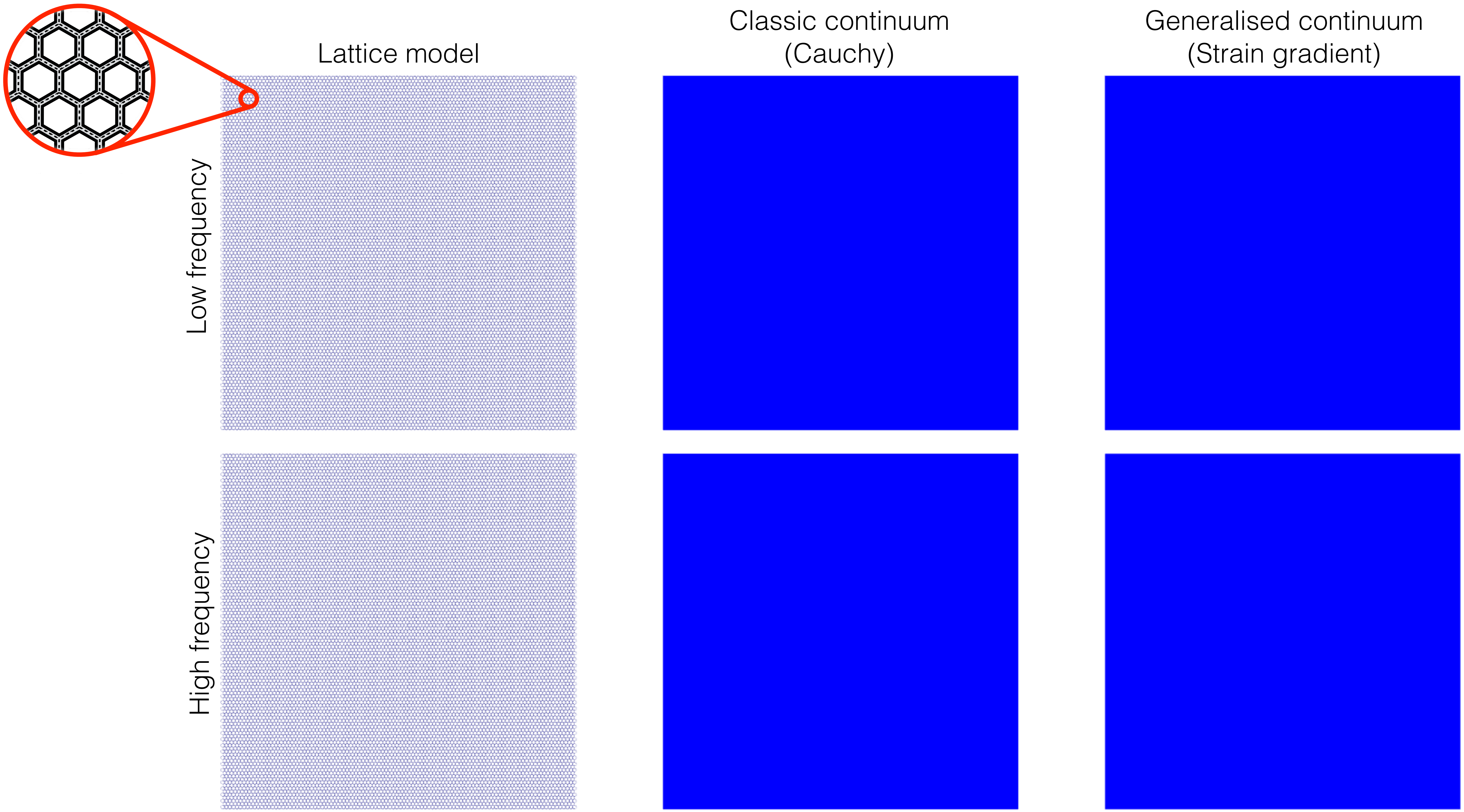

Wave propagation in architectured materials is not fully captured by a classic continuum

G. Rosi and N. Auffray, Continuum modelling of frequency dependent acoustic beam focusing and steering in hexagonal lattices, EJM/A

Wave propagation in hexagonal honeycombs

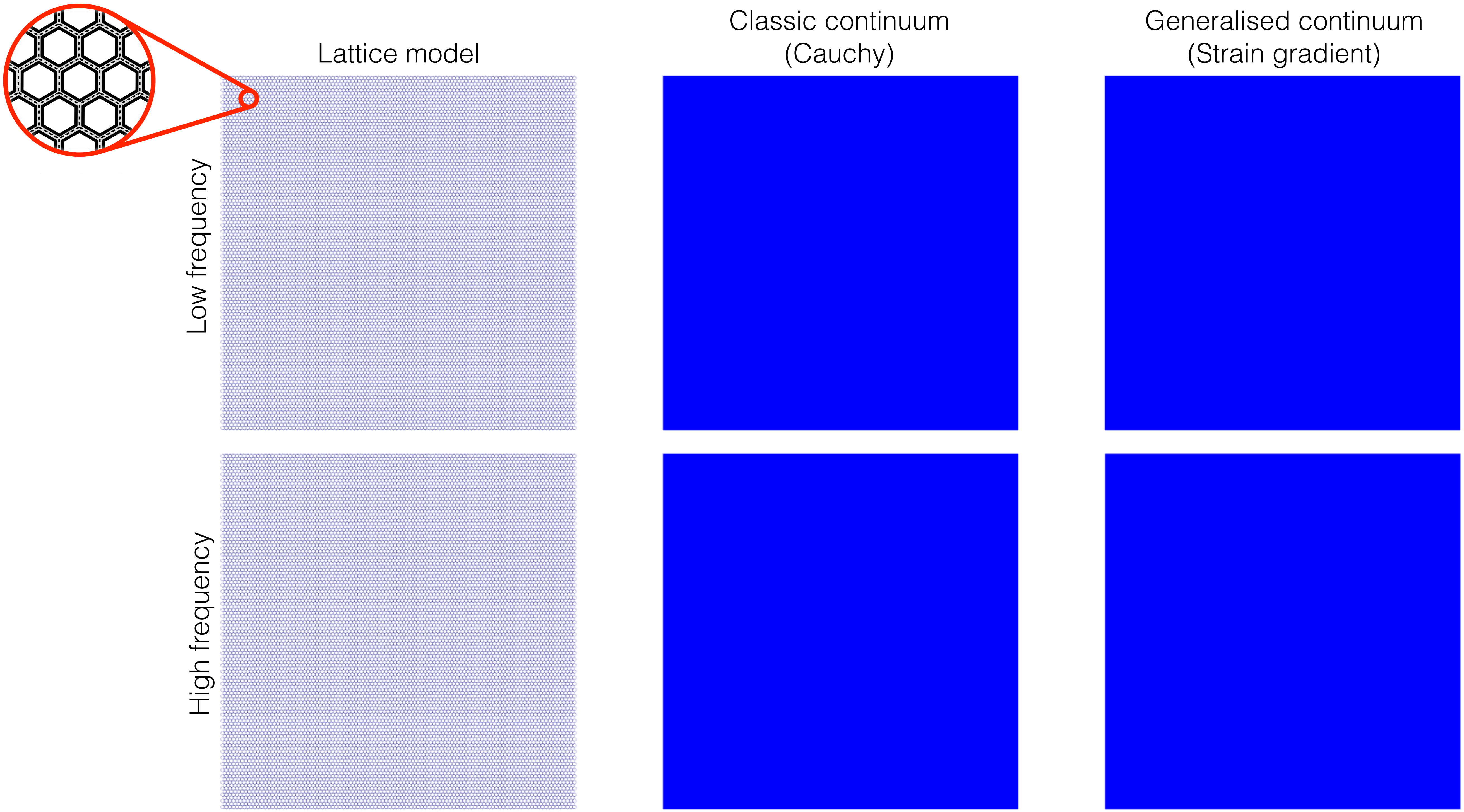

Wave propagation in architectured materials is not fully captured by a classic continuum

G. Rosi and N. Auffray, Continuum modelling of frequency dependent acoustic beam focusing and steering in hexagonal lattices, EJM/A

Wave propagation in hexagonal honeycombs

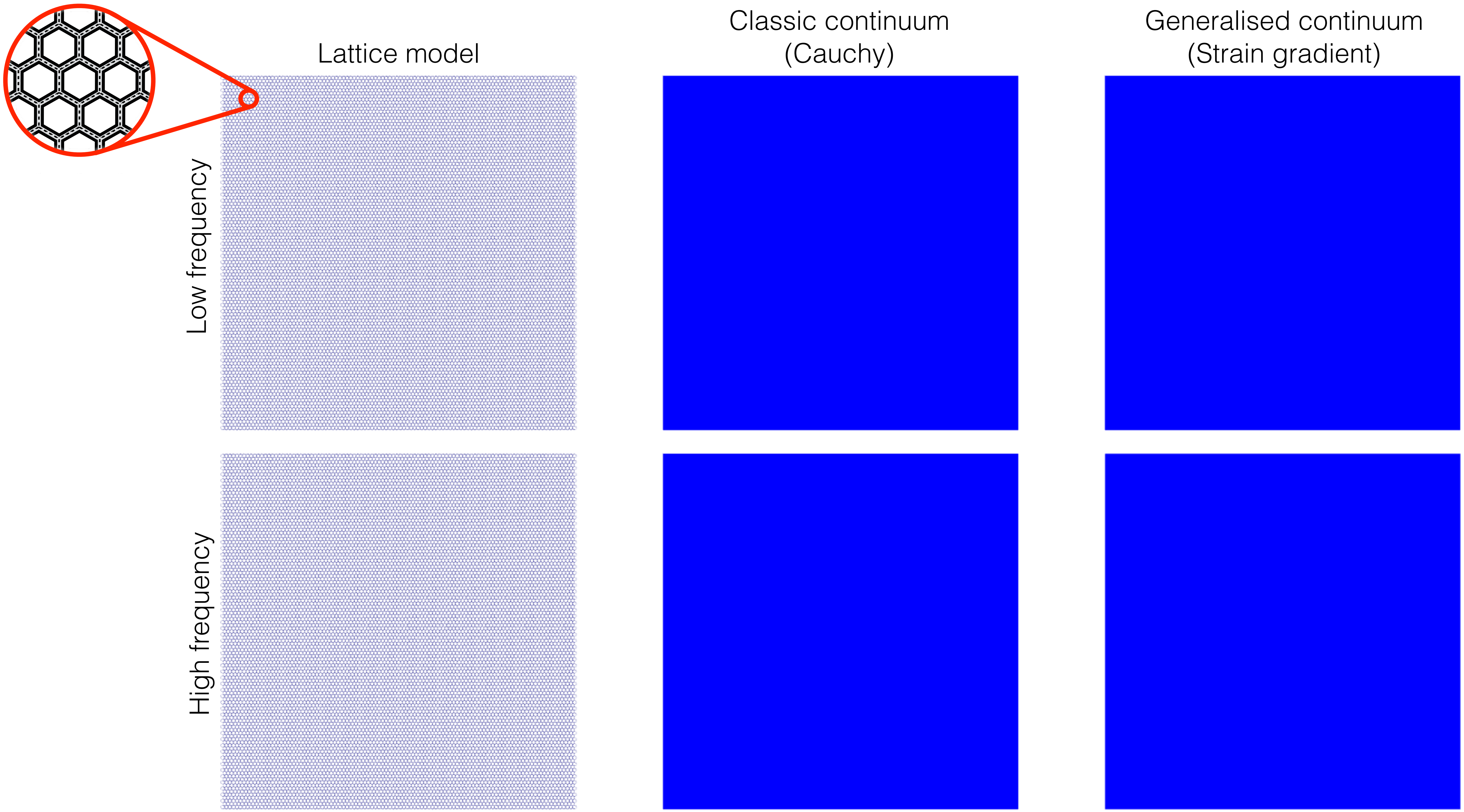

Wave propagation in architectured materials is not fully captured by a classic continuum

G. Rosi and N. Auffray, Continuum modelling of frequency dependent acoustic beam focusing and steering in hexagonal lattices, EJM/A

Wave propagation in gyroid lattices

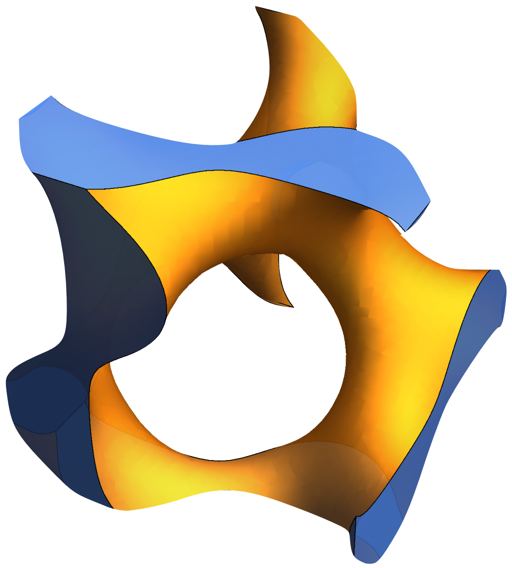

Triply periodic minimal surface

Simple equation :

$$\sin(a\pi x)\cos(a\pi y) + \cos(a\pi x)\sin(a\pi z) + \sin(a\pi y)\cos(a\pi z) = b$$

Two parameters a, b to control cell size and the porosity

Dolan et al. (2014). Optical Properties of Gyroid Structured Materials: From Photonic Crystals to Metamaterials. Advanced Optical Materials, 3(1), 12–32.

Wave propagation in gyroid lattices

Triply periodic minimal surface

Simple equation :

$$\sin(a\pi x)\cos(a\pi y) + \cos(a\pi x)\sin(a\pi z) + \sin(a\pi y)\cos(a\pi z) = b$$

Two parameters a, b to control cell size and the porosity

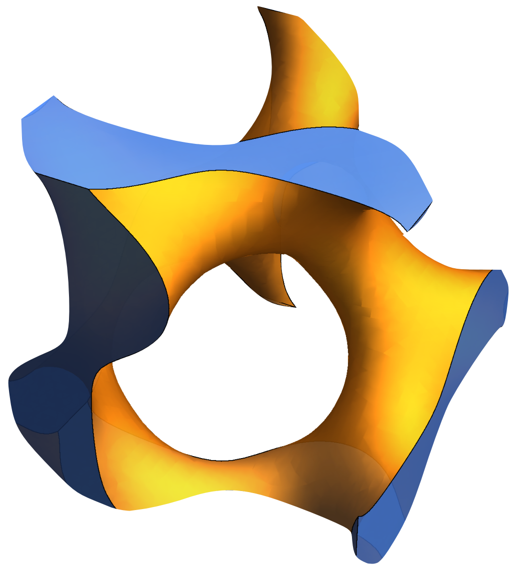

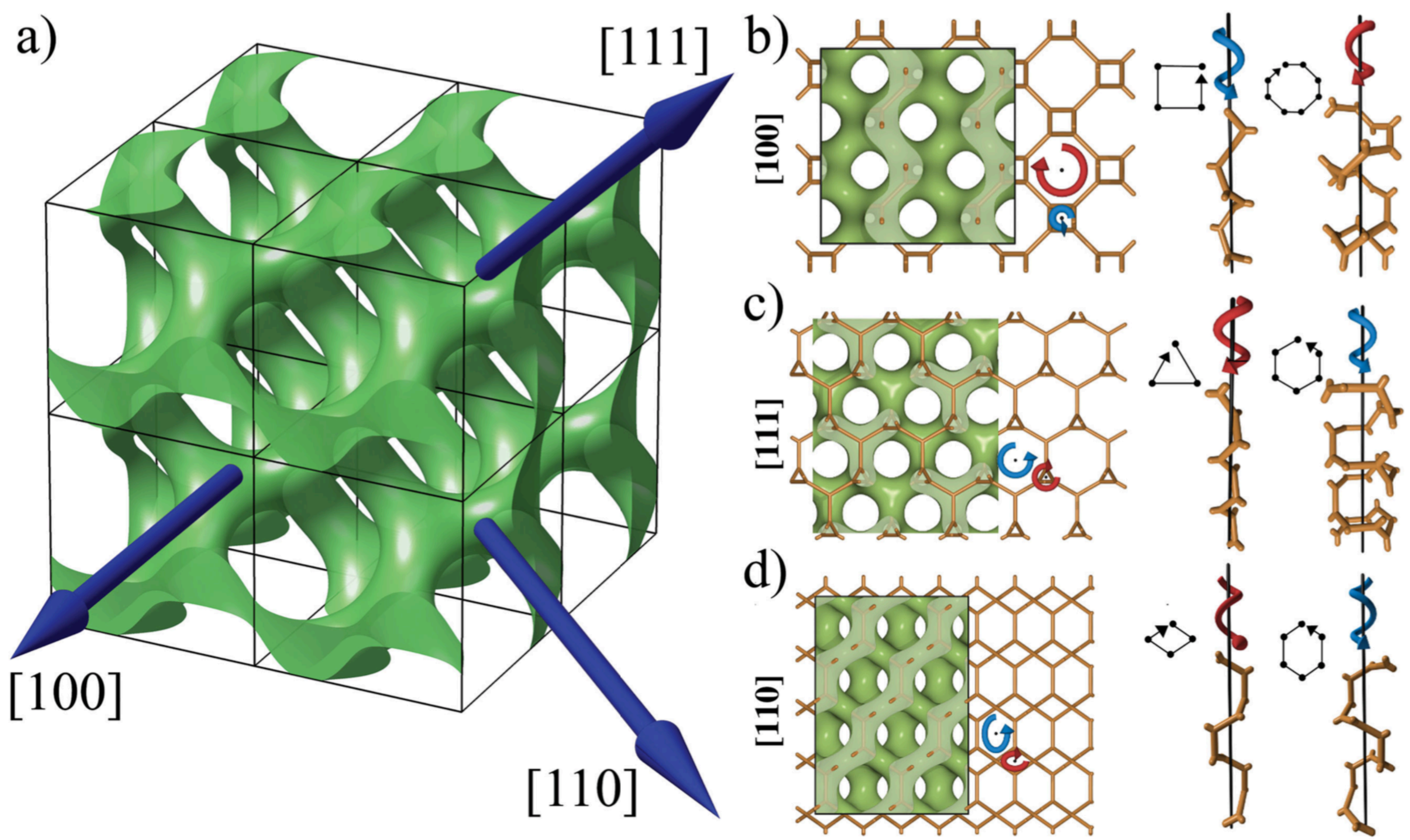

Dolan et al. (2014). Optical Properties of Gyroid Structured Materials: From Photonic Crystals to Metamaterials. Advanced Optical Materials, 3(1), 12–32.

Wave propagation in gyroid lattices

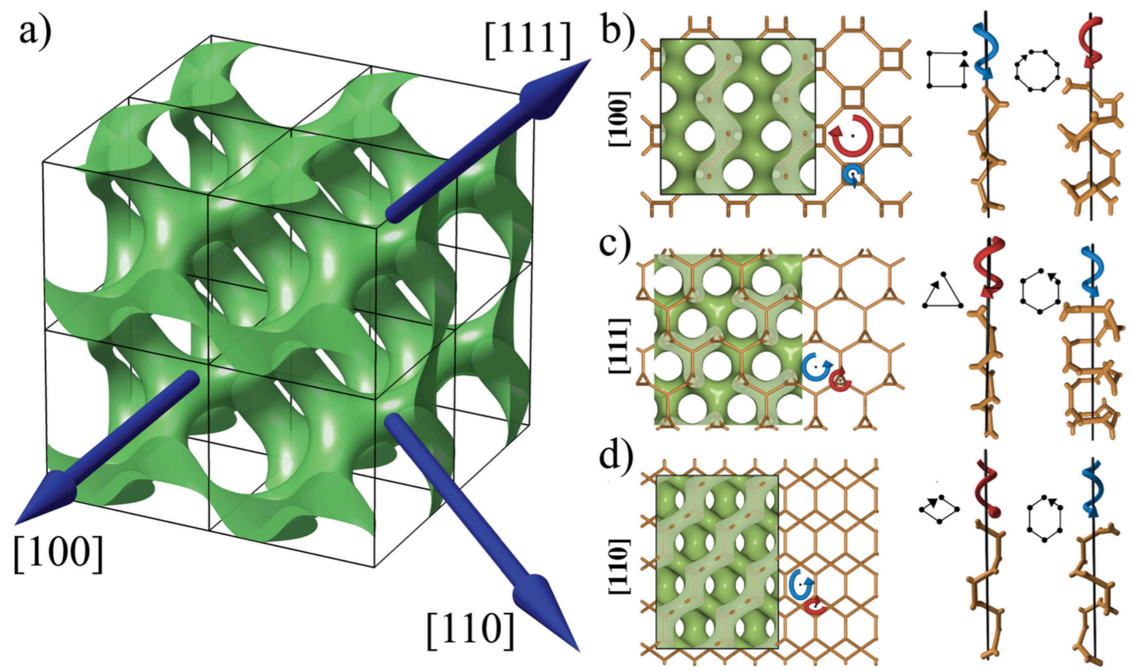

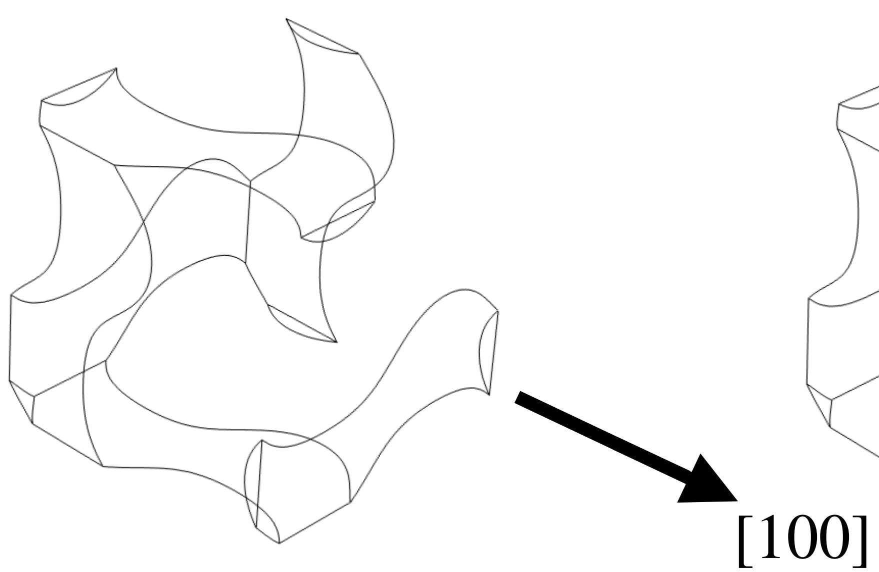

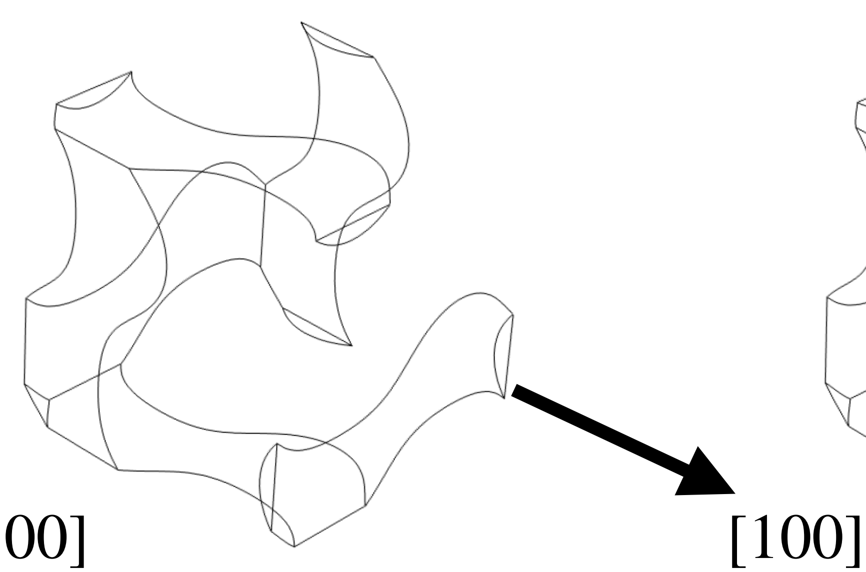

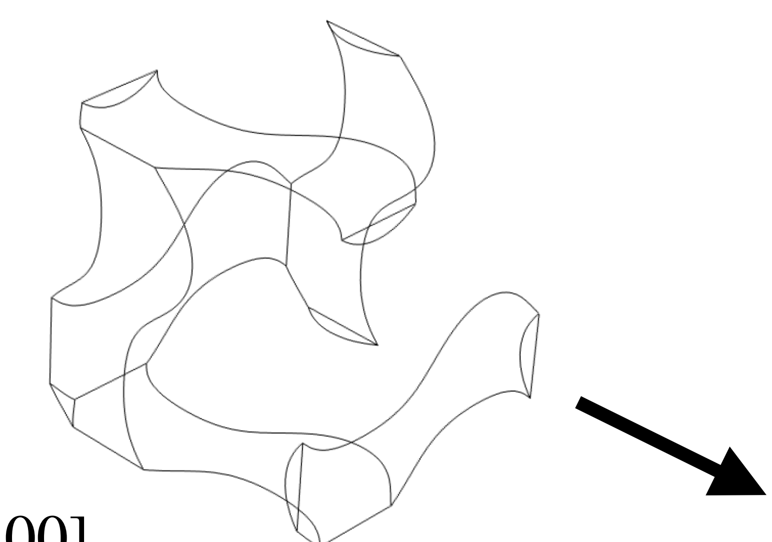

S_1 wave S_2 wave P wave [100]

Rosi, G., Auffray, N., Combescure, C. (2020). On the failure of classic elasticity in predicting elastic wave propagation in gyroid lattices for very long wavelengths. Symmetry

Wave propagation in gyroid lattices

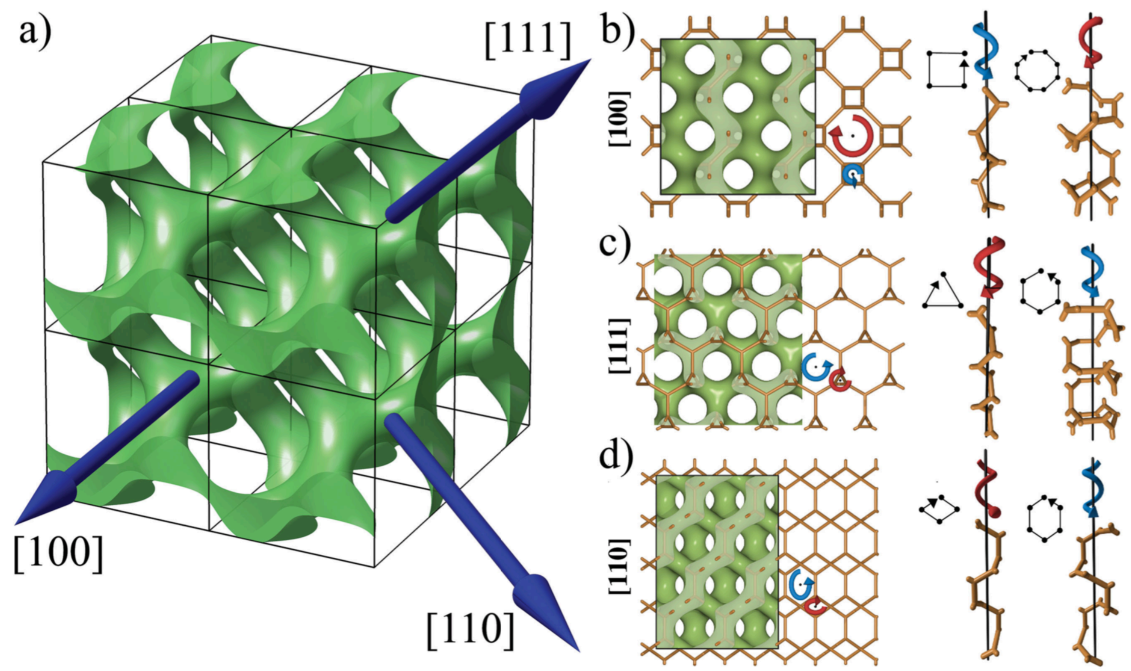

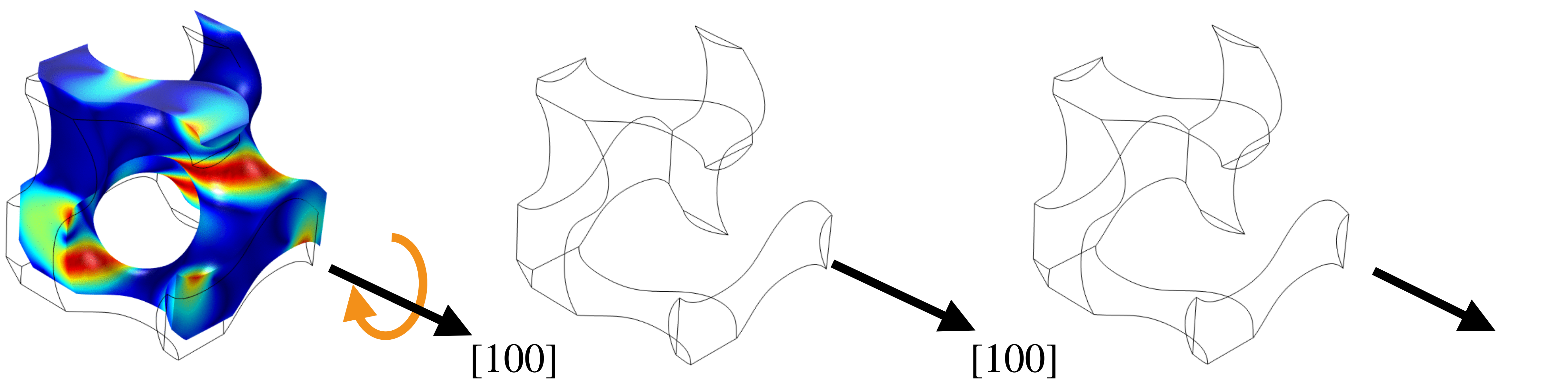

S_1 wave
Circular LH

S_2 wave

P wave

[100]

Rosi, G., Auffray, N., Combescure, C. (2020). On the failure of classic elasticity in predicting elastic wave propagation in gyroid lattices for very long wavelengths. Symmetry

Wave propagation in gyroid lattices

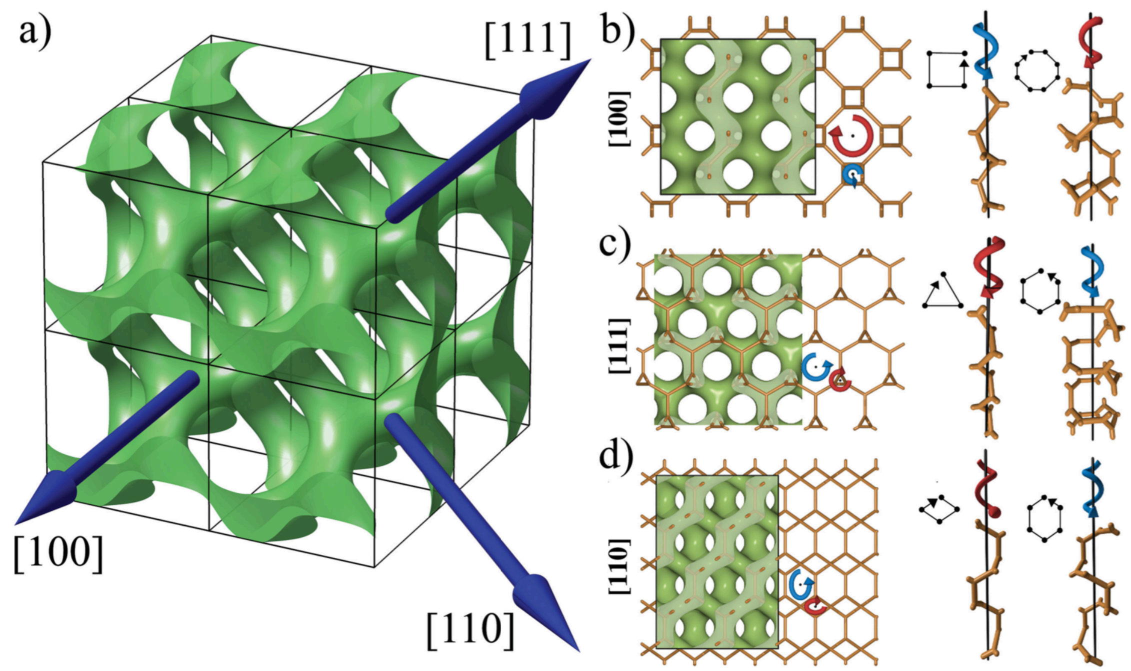

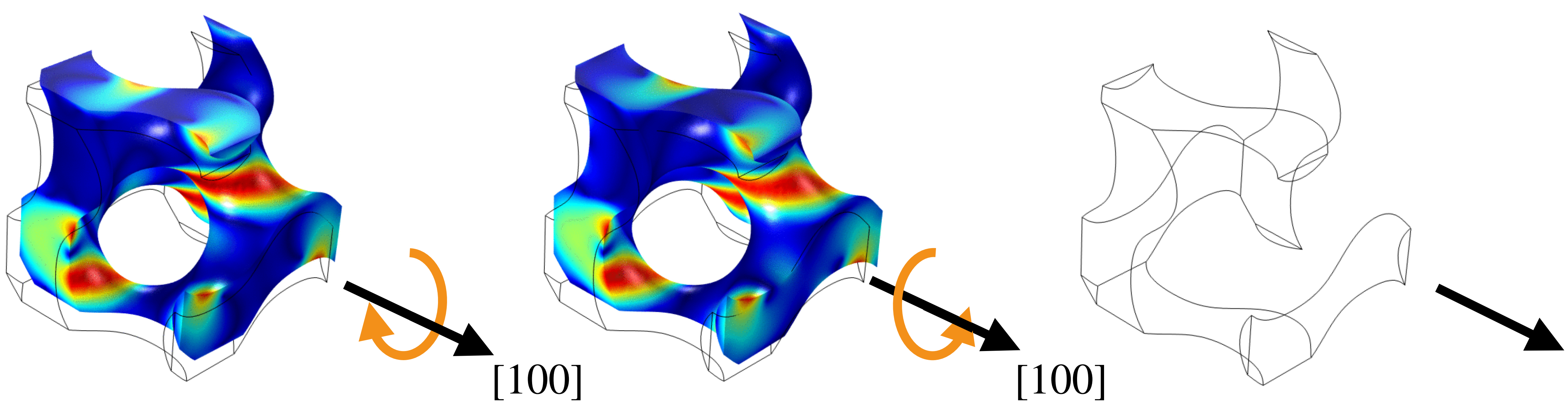

S_1 wave
Circular LH

S_2 wave
Circular RH

P wave

[100]

Rosi, G., Auffray, N., Combescure, C. (2020). On the failure of classic elasticity in predicting elastic wave propagation in gyroid lattices for very long wavelengths. Symmetry

Wave propagation in gyroid lattices

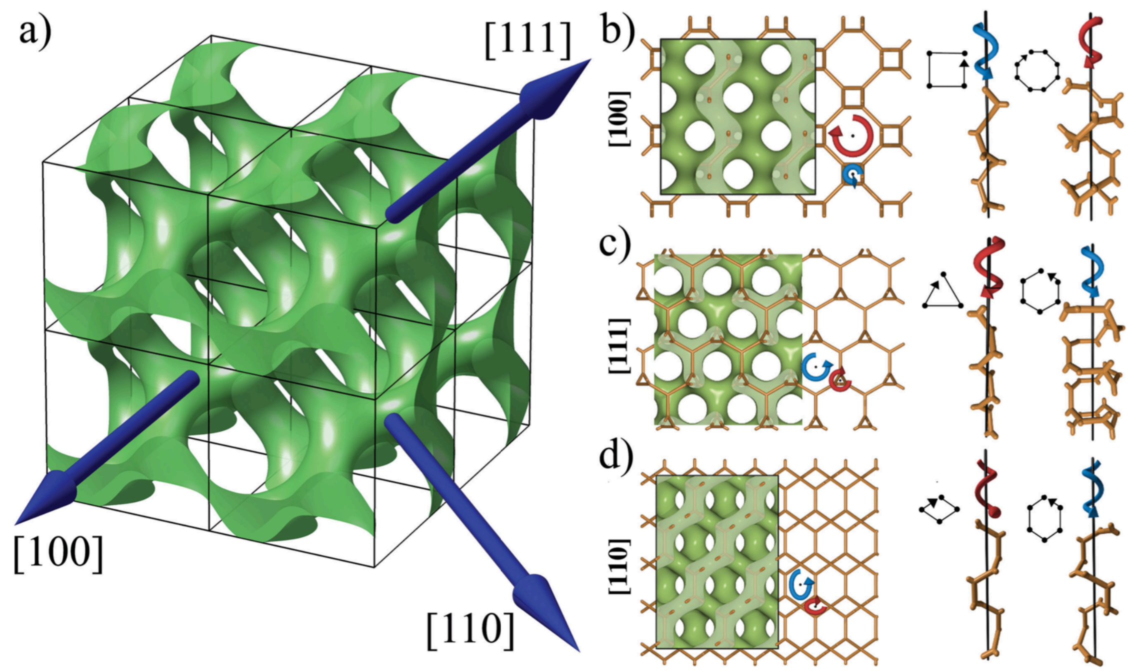

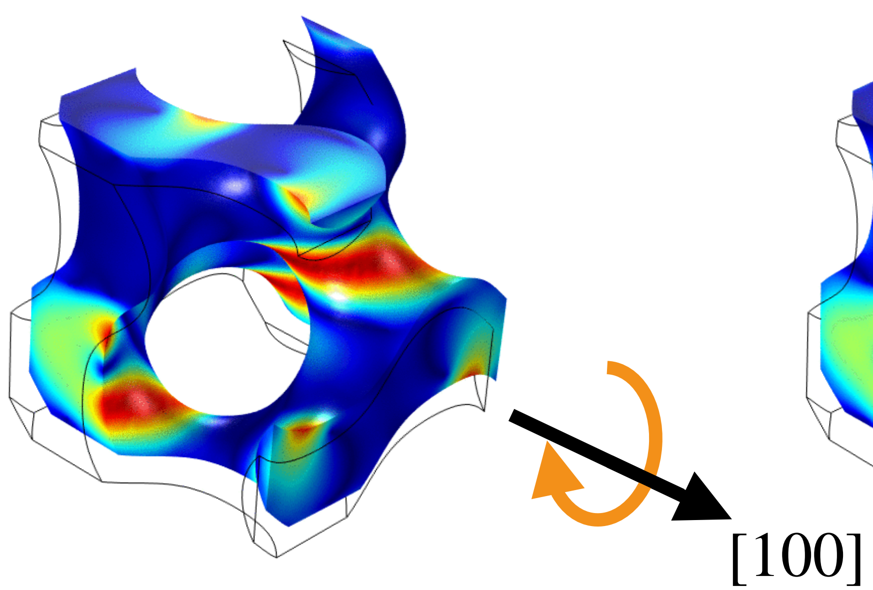

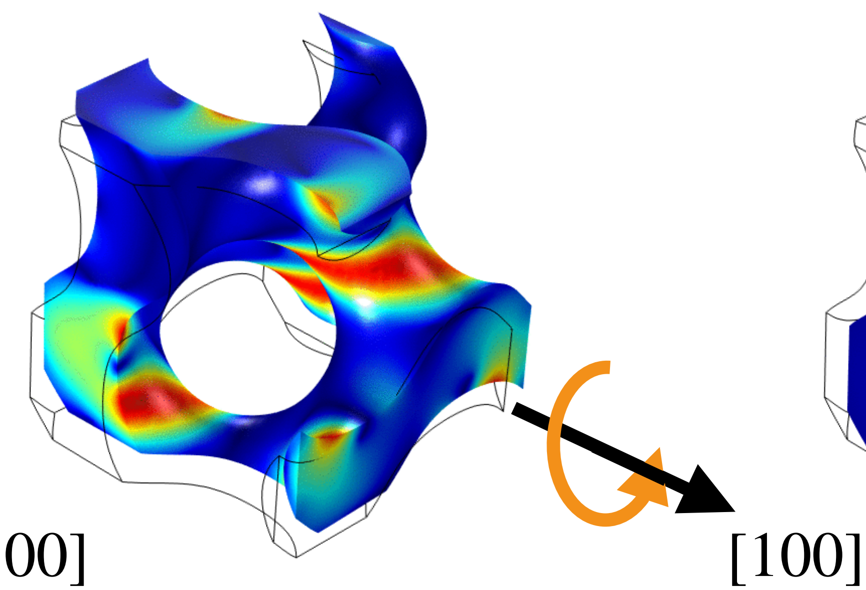

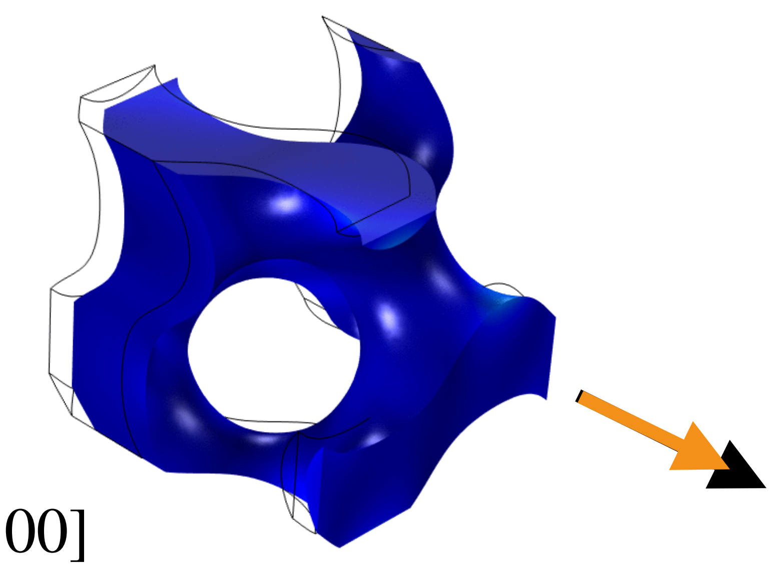

S_1 wave
Circular LH

S_2 wave
Circular RH

P wave
Linear

[100]

Rosi, G., Auffray, N., Combescure, C. (2020). On the failure of classic elasticity in predicting elastic wave propagation in gyroid lattices for very long wavelengths. Symmetry

Overview of the strain gradient model

Elastic energy

Strain tensor

$$\frac{1}{2}\left(\underset{\sim}{\sigma} : \underset{\sim}{\varepsilon}\right)$$

Stress tensor

Kinetic energy

Velocity

$$\frac{1}{2}\left(\underline{p} \cdot \dot{\underline{u}}\right)$$

Momentum

Balance equation

$$\nabla \cdot \left(\underset{\sim}{\sigma} \qquad\qquad \right) = \dot{\underline{p}}$$

Boundary conditions

Traction

$$\underline{t} = \left(\underset{\sim}{\sigma} \qquad\qquad\qquad \right) \underline{n}$$

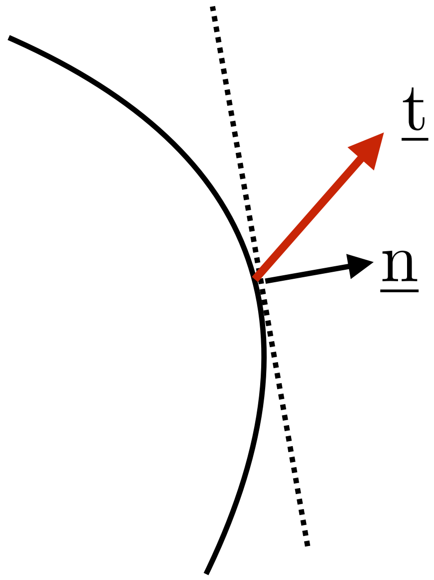

Overview of the strain gradient model

Elastic energy

Gradient of strain tensor

Strain tensor

$$\frac{1}{2}\left(\underset{\sim}{\sigma} : \underset{\sim}{\varepsilon}\right) + \frac{1}{2}\left(\underset{\approx}{\tau} \,\vdots\, \nabla \underset{\sim}{\varepsilon}\right)$$

Stress tensor

Hyper-Stress tensor

Kinetic energy

Velocity

$$\frac{1}{2}\left(\underline{p} \cdot \underline{\dot{u}}\right)$$

Momentum

Balance equation

$$\nabla \cdot \left(\underset{\sim}{\sigma} \qquad\qquad \right) = \underline{\dot{p}}$$

Boundary conditions

Traction

$$\underline{t} = \left(\underset{\sim}{\sigma} \qquad\qquad\qquad \right)\underline{n}$$

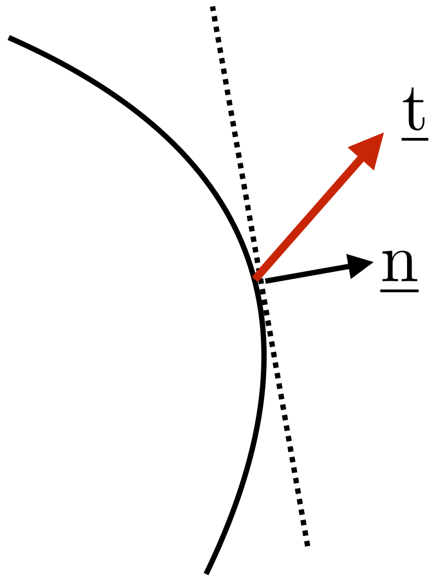

Overview of the strain gradient model

Elastic energy

Strain tensor — Gradient of strain tensor

$$\frac{1}{2}\left(\underset{\sim}{\sigma} : \underset{\sim}{\varepsilon}\right) + \frac{1}{2}\left(\underset{\approx}{\tau} \vdots \nabla \underset{\sim}{\varepsilon}\right)$$

Stress tensor — Hyper-Stress tensor

Kinetic energy

Velocity — Gradient of velocity

$$\frac{1}{2}\left(\underline{p} \cdot \dot{\underline{u}}\right) + \frac{1}{2}\left(\underset{\sim}{q} : \nabla \dot{\underline{u}}\right)$$

Momentum — Hyper momentum

Balance equation

$$\nabla \cdot \left(\underset{\sim}{\sigma} \qquad \right) = \dot{\underline{p}}$$

Boundary conditions

Traction

$$\underline{t} = \left(\underset{\sim}{\sigma} \qquad \right) \underline{n}$$

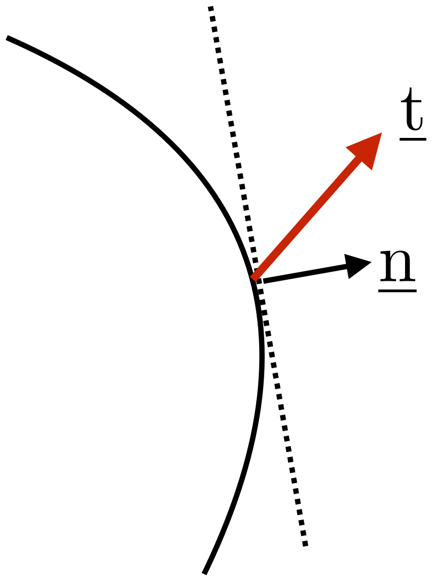

Overview of the strain gradient model

Elastic energy

Strain tensor — Gradient of strain tensor

$$\frac{1}{2}\left(\underset{\sim}{\sigma} : \underset{\sim}{\varepsilon}\right) + \frac{1}{2}\left(\underset{\approx}{\tau} \,\vdots\, \nabla \underset{\sim}{\varepsilon}\right)$$

Stress tensor — Hyper-Stress tensor

Kinetic energy

Velocity — Gradient of velocity

$$\frac{1}{2}\left(\underline{p} \cdot \dot{\underline{u}}\right) + \frac{1}{2}\left(\underset{\sim}{q} : \nabla \dot{\underline{u}}\right)$$

Momentum — Hyper momentum

Balance equation

$$\nabla \cdot \left(\underset{\sim}{\sigma} - \nabla \cdot \underset{\approx}{\tau}\right) = \dot{\underline{p}} - \nabla \cdot \dot{\underset{\sim}{q}}$$

Boundary conditions

Traction

$$\underline{t} = \left(\underset{\sim}{\sigma} \qquad\qquad\qquad\qquad \right)\underline{n}$$

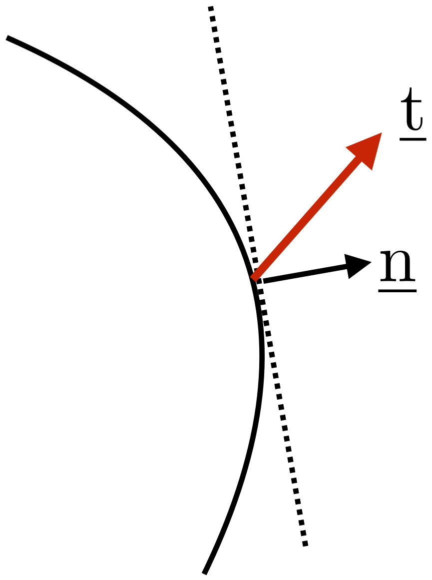

Overview of the strain gradient model

Elastic energy

Strain tensor — Gradient of strain tensor

$$\frac{1}{2}\left(\underset{\sim}{\sigma} : \underset{\sim}{\varepsilon}\right) + \frac{1}{2}\left(\underset{\approx}{\tau} \,\vdots\, \nabla \underset{\sim}{\varepsilon}\right)$$

Stress tensor — Hyper-Stress tensor

Kinetic energy

Velocity — Gradient of velocity

$$\frac{1}{2}\left(\underline{p} \cdot \dot{\underline{u}}\right) + \frac{1}{2}\left(\underset{\sim}{q} : \nabla \dot{\underline{u}}\right)$$

Momentum — Hyper momentum

Balance equation

$$\nabla \cdot \left(\underset{\sim}{\sigma} - \nabla \cdot \underset{\approx}{\tau}\right) = \dot{\underline{p}} - \nabla \cdot \dot{\underset{\sim}{q}}$$

Boundary conditions

Traction

$$\underline{t} = \left(\underset{\sim}{\sigma} - \nabla \cdot \underset{\approx}{\tau} + \dot{\underset{\sim}{q}}\right)\underline{n} + \nabla^{S} \cdot \left(\underset{\approx}{\tau}\,\underline{n}\right)$$

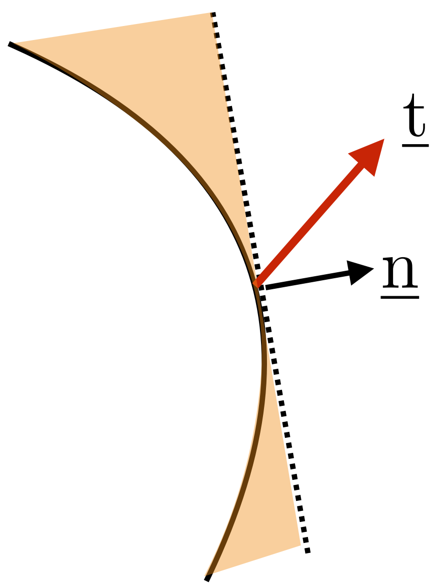

Overview of the strain gradient model

Elastic energy

$$\frac{1}{2}\left(\underset{\sim}{\sigma} : \underset{\sim}{\varepsilon}\right) + \frac{1}{2}\left(\underset{\approx}{\tau} \vdots \nabla \underset{\sim}{\varepsilon}\right)$$

Strain tensor; Gradient of strain tensor; Stress tensor; Hyper-Stress tensor

Kinetic energy

$$\frac{1}{2}\left(\underline{p} \cdot \underline{\dot{u}}\right) + \frac{1}{2}\left(\underset{\sim}{q} : \nabla \underline{\dot{u}}\right)$$

Velocity; Gradient of velocity; Momentum; Hyper momentum

Balance equation

$$\nabla \cdot \left(\underset{\sim}{\sigma} - \nabla \cdot \underset{\approx}{\tau}\right) = \underline{\dot{p}} - \nabla \cdot \underset{\sim}{\dot{q}}$$

Boundary conditions

Traction

$$\underline{t} = \left(\underset{\sim}{\sigma} - \nabla \cdot \underset{\sim}{\tau} + \underset{\sim}{\dot{q}}\right)\underline{n} + \nabla^{S} \cdot \left(\underset{\approx}{\tau}\underline{n}\right)$$

Hyper traction

$$\underline{R} = \left(\underset{\approx}{\tau}\underline{n}\right)\underline{n}$$

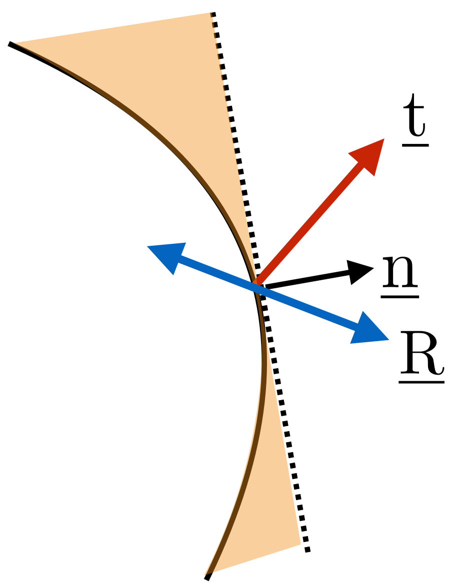

Overview of the strain gradient model

Elastic energy

Strain tensor — Gradient of strain tensor

$$\frac{1}{2}\left(\underset{\sim}{\sigma} : \underset{\sim}{\varepsilon}\right) + \frac{1}{2}\left(\underset{\approx}{\tau} \vdots \nabla \underset{\sim}{\varepsilon}\right)$$

Stress tensor — Hyper-Stress tensor

Kinetic energy

Velocity — Gradient of velocity

$$\frac{1}{2}\left(\underline{p} \cdot \dot{\underline{u}}\right) + \frac{1}{2}\left(\underset{\sim}{q} : \nabla \dot{\underline{u}}\right)$$

Momentum — Hyper momentum

Balance equation

$$\nabla \cdot \left(\underset{\sim}{\sigma} - \nabla \cdot \underset{\approx}{\tau}\right) = \dot{\underline{p}} - \nabla \cdot \dot{\underset{\sim}{q}}$$

Boundary conditions

Traction

$$\underline{t} = \left(\underset{\sim}{\sigma} - \nabla \cdot \underset{\sim}{\tau} + \dot{\underset{\sim}{q}}\right)\underline{n} + \nabla^{S} \cdot \left(\underset{\approx}{\tau}\,\underline{n}\right)$$

Hyper traction

$$\underline{R} = \left(\underset{\approx}{\tau}\,\underline{n}\right)\underline{n}$$

Edge (wedge) forces

$$\underline{\nu} = [[\underline{\tau}\,\underline{n}_1 \otimes \underline{n}_2]]$$

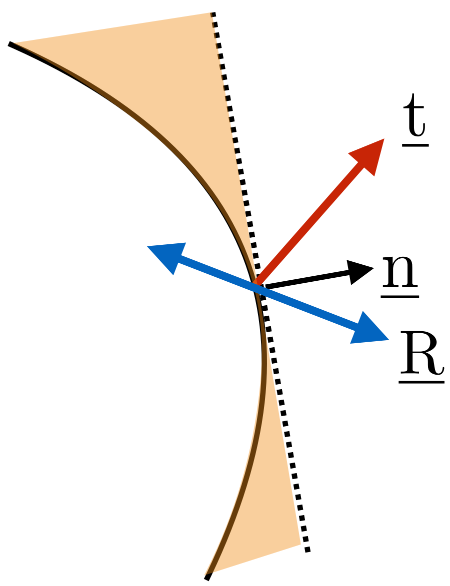

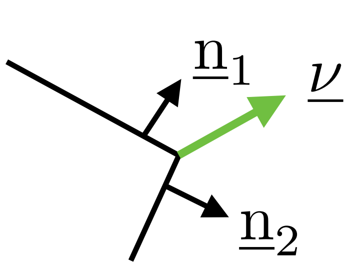

Constitutive equations

The complete set of constitutive equations is

$$\begin{pmatrix} \underline{\mathrm{p}} \\ \underset{\sim}{\mathrm{q}} \\ \underset{\sim}{\sigma} \\ \underset{\simeq}{\tau} \end{pmatrix} = \begin{pmatrix} \rho \underset{\sim}{\mathrm{I}} & \underset{\simeq}{\mathrm{K}} & 0 & 0 \\ \underset{\simeq}{\mathrm{K}}^T & \underset{\approx}{\mathrm{J}} & 0 & 0 \\ 0 & 0 & \underset{\approx}{\mathrm{C}} & \underset{\approx}{\mathrm{M}} \\ 0 & 0 & \underset{\approx}{\mathrm{M}}^T & \underset{\approx}{\mathrm{A}} \end{pmatrix} \begin{pmatrix} \underline{\mathrm{v}} \\ \underset{\sim}{\nabla \mathrm{v}} \\ \underset{\sim}{\varepsilon} \\ \underset{\simeq}{\eta} \end{pmatrix}$$

	Symmetry classes	Dispersion	Non centrosymmetry	Chirality

Constitutive equations

The complete set of constitutive equations is

$$\begin{pmatrix} \underline{p} \\ \underset{\sim}{q} \\ \underset{\sim}{\sigma} \\ \underset{\approx}{\tau} \end{pmatrix} = \begin{pmatrix} \rho \underset{\sim}{I} & \underset{\approx}{K} & 0 & 0 \\ \underset{\approx}{K}^T & \underset{\approx}{J} & 0 & 0 \\ 0 & 0 & \underset{\approx}{C} & \underset{\approx}{M} \\ 0 & 0 & \underset{\approx}{M}^T & \underset{\approx}{A} \end{pmatrix} \begin{pmatrix} \underline{v} \\ \nabla \underset{\sim}{v} \\ \underset{\sim}{\varepsilon} \\ \underset{\approx}{\eta} \end{pmatrix}$$

		Symmetry classes	Dispersion	Non centrosymmetry	Chirality
macroscopic mass density	$\rho I_{(ij)}$	2	✗	✗	✗
classical elasticity	$C_{\underline{(ij)}\,\underline{(kl)}}$	8	✗	✗	✗

Constitutive equations

The complete set of constitutive equations is

$$\begin{pmatrix} \underline{p} \\ \underset{\sim}{q} \\ \underset{\sim}{\sigma} \\ \underset{\approx}{\tau} \end{pmatrix} = \begin{pmatrix} \rho \underset{\sim}{I} & \underset{\simeq}{K} & 0 & 0 \\ \underset{\simeq}{K}^T & \underset{\approx}{J} & 0 & 0 \\ 0 & 0 & \underset{\approx}{C} & \underset{\approx}{M} \\ 0 & 0 & \underset{\approx}{M}^T & \underset{\approx}{A} \end{pmatrix} \begin{pmatrix} \underline{v} \\ \nabla \underset{\sim}{v} \\ \underset{\sim}{\varepsilon} \\ \underset{\simeq}{\eta} \end{pmatrix}$$

		Symmetry classes	Dispersion	Non centrosymmetry	Chirality
macroscopic mass density	$\rho I_{(ij)}$	2	✗	✗	✗
classical elasticity	$C_{\underline{(ij)}\,\underline{(kl)}}$	8	✗	✗	✗
second order inertia	$J_{\underline{(ij)}\,\underline{(kl)}}$	8	✓	✗	✗
second order elasticity	$A_{\underline{(ij)k}\,\underline{(lm)n}}$	17	✓	✗	✗

Auffray et al (2018). JMPS

Constitutive equations

The complete set of constitutive equations is

$$\begin{pmatrix} \underline{\mathrm{p}} \\ \underset{\sim}{\mathrm{q}} \\ \underset{\sim}{\sigma} \\ \underset{\simeq}{\tau} \end{pmatrix} = \begin{pmatrix} \rho \underset{\sim}{\mathrm{I}} & \underset{\simeq}{\mathrm{K}} & 0 & 0 \\ \underset{\simeq}{\mathrm{K}}^T & \underset{\approx}{\mathrm{J}} & 0 & 0 \\ 0 & 0 & \underset{\approx}{\mathrm{C}} & \underset{\approx}{\mathrm{M}} \\ 0 & 0 & \underset{\approx}{\mathrm{M}}^T & \underset{\approx}{\mathrm{A}} \end{pmatrix} \begin{pmatrix} \underline{\mathrm{v}} \\ \underset{\sim}{\nabla \mathrm{v}} \\ \underset{\sim}{\varepsilon} \\ \underset{\simeq}{\eta} \end{pmatrix}$$

		Symmetry classes	Dispersion	Non centrosymmetry	Chirality
macroscopic mass density	$\rho I_{(ij)}$	2	✗	✗	✗
classical elasticity	$C_{\underline{(ij)}\,\underline{(kl)}}$	8	✗	✗	✗
second order inertia	$J_{\underline{(ij)}\,\underline{(kl)}}$	8	✓	✗	✗
second order elasticity	$A_{\underline{(ij)k}\;\underline{(lm)n}}$	17	✓	✗	✗
coupling inertia	K_{ijk}	17	✓	✓	✓
coupling elasticity	$M_{(ij)(lm)n}$	29	✓	✓	✓

Auffray et al (2018). JMPS

Constitutive equations

The complete set of constitutive equations is

$$\begin{pmatrix} \underline{\mathrm{p}} \\ \underset{\sim}{\mathrm{q}} \\ \underset{\sim}{\sigma} \\ \underset{\approx}{\tau} \end{pmatrix} = \begin{pmatrix} \rho \underset{\sim}{\mathrm{I}} & \underset{\approx}{\mathrm{K}} & 0 & 0 \\ \underset{\approx}{\mathrm{K}}^T & \underset{\approx}{\mathrm{J}} & 0 & 0 \\ 0 & 0 & \underset{\approx}{\mathrm{C}} & \underset{\approx}{\mathrm{M}} \\ 0 & 0 & \underset{\approx}{\mathrm{M}}^T & \underset{\underset{\sim}{\approx}}{\mathrm{A}} \end{pmatrix} \begin{pmatrix} \underline{\mathrm{v}} \\ \underset{\sim}{\nabla \mathrm{v}} \\ \underset{\sim}{\varepsilon} \\ \underset{\approx}{\eta} \end{pmatrix}$$

		Symmetry classes	Dispersion	Non centrosymmetry	Chirality
macroscopic mass density	$\rho I_{(ij)}$	2	✗	✗	✗
classical elasticity	$C_{\underline{(ij)}\,\underline{(kl)}}$	8	✗	✗	✗
second order inertia	$J_{\underline{(ij)}\,\underline{(kl)}}$	8	✓	✗	✗
second order elasticity	$A_{\underline{(ij)k}\,\underline{(lm)n}}$	17	✓	✗	✗
coupling inertia	K_{ijk}	17	✓	✓	✓
coupling elasticity	$M_{(ij)(lm)n}$	29	✓	✓	✓

a total of 48 classes

Auffray et al (2018). JMPS

Hexagonal honeycomb in 2D plane strain

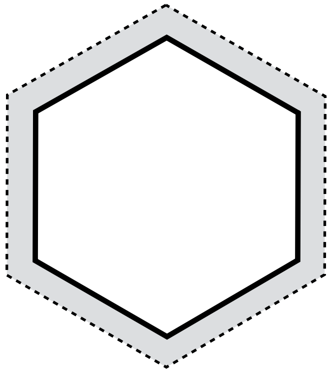

$$\begin{pmatrix} \underline{p} \\ \underset{\sim}{q} \\ \underset{\sim}{\sigma} \\ \underset{\simeq}{\tau} \end{pmatrix} = \begin{pmatrix} \rho \underset{\sim}{I} & \underset{\simeq}{K} & 0 & 0 \\ \underset{\simeq}{K}^T & \underset{\approx}{J} & 0 & 0 \\ 0 & 0 & \underset{\approx}{C} & \underset{\approx}{M} \\ 0 & 0 & \underset{\approx}{M}^T & \underset{\underset{\sim}{\approx}}{A} \end{pmatrix} \begin{pmatrix} \underline{v} \\ \nabla \underset{\sim}{v} \\ \underset{\sim}{\varepsilon} \\ \underset{\simeq}{\eta} \end{pmatrix}$$

Hexagonal honeycomb in 2D plane strain

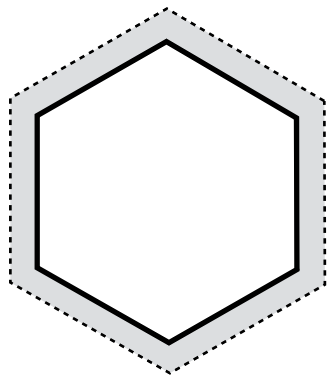

Six rotational symmetries

$$
\begin{pmatrix} \underline{p} \\ \underset{\sim}{q} \\ \underset{\sim}{\sigma} \\ \underset{\simeq}{\tau} \end{pmatrix}
=
\begin{pmatrix}
\rho \underset{\sim}{I} & \underset{\simeq}{K} & 0 & 0 \\
\underset{\simeq}{K}^T & \underset{\approx}{J} & 0 & 0 \\
0 & 0 & \underset{\approx}{C} & \underset{\approx}{M} \\
0 & 0 & \underset{\approx}{M}^T & \underset{\underset{\sim}{\approx}}{A}
\end{pmatrix}
\begin{pmatrix} \underline{v} \\ \nabla \underset{\sim}{v} \\ \underset{\sim}{\varepsilon} \\ \underset{\simeq}{\eta} \end{pmatrix}
$$

Hexagonal honeycomb in 2D plane strain

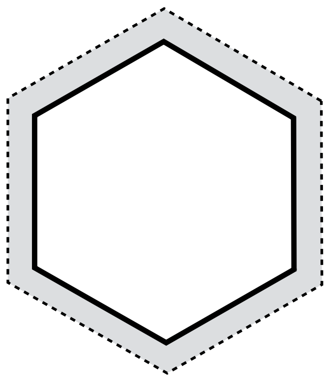

Six rotational symmetries

Six mirror planes

$$\begin{pmatrix} \underline{p} \\ \underset{\sim}{q} \\ \underset{\sim}{\sigma} \\ \underset{\simeq}{\tau} \end{pmatrix} = \begin{pmatrix} \rho \underset{\sim}{I} & \underset{\simeq}{K} & 0 & 0 \\ \underset{\simeq}{K}^T & \underset{\approx}{J} & 0 & 0 \\ 0 & 0 & \underset{\approx}{C} & \underset{\approx}{M} \\ 0 & 0 & \underset{\approx}{M}^T & \underset{\underset{\sim}{\approx}}{A} \end{pmatrix} \begin{pmatrix} \underline{v} \\ \underset{\sim}{\nabla \underline{v}} \\ \underset{\sim}{\varepsilon} \\ \underset{\simeq}{\eta} \end{pmatrix}$$

Hexagonal honeycomb in 2D plane strain

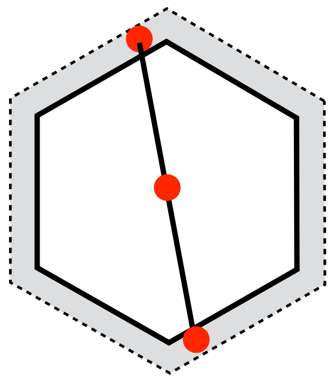

Six rotational symmetries

Six mirror planes

A center of symmetry

$$\begin{pmatrix} \underline{p} \\ \underset{\sim}{q} \\ \underset{\sim}{\sigma} \\ \underset{\approx}{\tau} \end{pmatrix} = \begin{pmatrix} \rho \underset{\sim}{I} & \cancel{\underset{\approx}{M}} & 0 & 0 \\ \cancel{\underline{K}^T} & \underset{\approx}{J} & 0 & 0 \\ 0 & 0 & \underset{\approx}{C} & \cancel{\underset{\approx}{M}} \\ 0 & 0 & \cancel{\underset{\approx}{M}^T} & \underset{\approx}{A} \end{pmatrix} \begin{pmatrix} \underline{v} \\ \nabla \underset{\sim}{v} \\ \underset{\sim}{\varepsilon} \\ \underset{\approx}{\eta} \end{pmatrix}$$

Hexagonal honeycomb in 2D plane strain

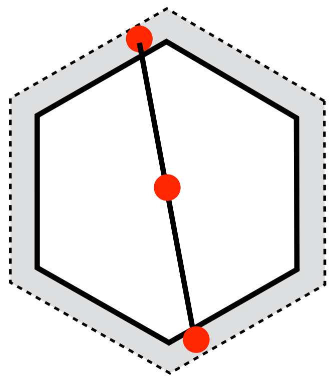

Six rotational symmetries

Six mirror planes

A center of symmetry

$$
\begin{pmatrix} \underline{p} \\ \underset{\sim}{q} \\ \underset{\sim}{\sigma} \\ \underset{\approx}{\tau} \end{pmatrix}
=
\begin{pmatrix}
\rho \underset{\sim}{I} & \cancel{\underset{\approx}{K}} & 0 & 0 \\
\cancel{\underline{K}^T} & \underset{\approx}{J} & 0 & 0 \\
0 & 0 & \underset{\approx}{C} & \cancel{\underset{\approx}{M}} \\
0 & 0 & \cancel{\underline{M}^T} & \underset{\approx}{A}
\end{pmatrix}
\begin{pmatrix} \underline{v} \\ \nabla \underset{\sim}{v} \\ \underset{\sim}{\varepsilon} \\ \underset{\approx}{\eta} \end{pmatrix}
$$

The generalised Christoffel equation for the directions $\theta = 0°$ and $\theta = 30°$ gives the following phase velocities

$\theta = 0°$

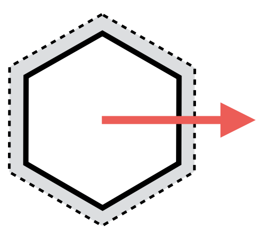

$$v_p(k) = \sqrt{\frac{c_P + (a_P + a_D)k^2}{\rho + J_P k^2}}$$

$$v_s(k) = \sqrt{\frac{c_S + a_S k^2}{\rho + J_S k^2}}$$

Hexagonal honeycomb in 2D plane strain

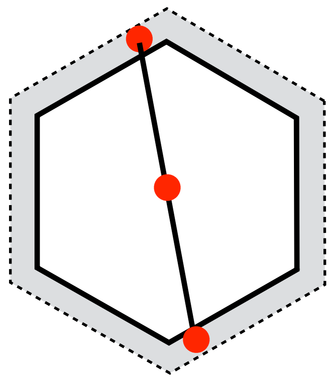

Six rotational symmetries

Six mirror planes

A center of symmetry

$$\begin{pmatrix} \underline{p} \\ \underset{\sim}{q} \\ \underset{\sim}{\sigma} \\ \underset{\approx}{\tau} \end{pmatrix} = \begin{pmatrix} \rho \underset{\sim}{I} & \underset{\approx}{K} & 0 & 0 \\ \underset{\approx}{K}^T & \underset{\approx}{J} & 0 & 0 \\ 0 & 0 & \underset{\approx}{C} & \underset{\approx}{M} \\ 0 & 0 & \underset{\approx}{M}^T & \underset{\approx}{A} \end{pmatrix} \begin{pmatrix} \underline{v} \\ \nabla \underset{\sim}{v} \\ \underset{\sim}{\varepsilon} \\ \underset{\approx}{\eta} \end{pmatrix}$$

The generalised Christoffel equation for the directions $\theta = 0°$ and $\theta = 30°$ gives the following phase velocities

$\theta = 0°$

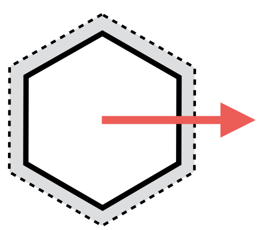

$\theta = 30°$

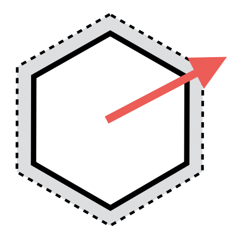

$$v_p(k) = \sqrt{\frac{c_P + (a_P + a_D)k^2}{\rho + J_P k^2}} \qquad v_p(k) = \sqrt{\frac{c_P + a_P k^2}{\rho + J_P k^2}}$$

$$v_s(k) = \sqrt{\frac{c_S + a_S k^2}{\rho + J_S k^2}} \qquad v_s(k) = \sqrt{\frac{c_S + (a_S + a_D)k^2}{\rho + J_S k^2}}$$

Hexagonal honeycomb in 2D plane strain

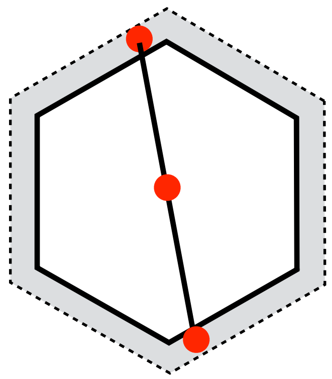

Six rotational symmetries

Six mirror planes

A center of symmetry

$$\begin{pmatrix} \underline{p} \\ \underset{\sim}{q} \\ \underset{\sim}{\sigma} \\ \underset{\approx}{\tau} \end{pmatrix} = \begin{pmatrix} \rho \underset{\sim}{I} & \cancel{\underset{\approx}{K}} & 0 & 0 \\ \cancel{\underset{\approx}{K}^T} & \underset{\approx}{J} & 0 & 0 \\ 0 & 0 & \underset{\approx}{C} & \cancel{\underset{\approx}{M}} \\ 0 & 0 & \cancel{\underset{\approx}{M}^T} & \underset{\approx}{A} \end{pmatrix} \begin{pmatrix} \underline{v} \\ \nabla \underset{\sim}{v} \\ \underset{\sim}{\varepsilon} \\ \underset{\approx}{\eta} \end{pmatrix}$$

The generalised Christoffel equation for the directions $\theta = 0°$ and $\theta = 30°$ gives the following phase velocities

$\theta = 0°$

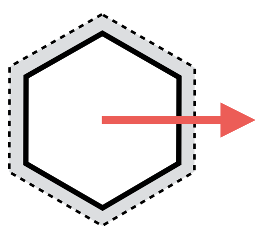

$\theta = 30°$

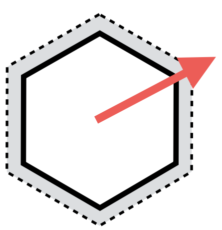

$$v_p(k) = \sqrt{\frac{c_P + (a_P + a_D)k^2}{\rho + J_P k^2}} \qquad v_p(k) = \sqrt{\frac{c_P + a_P k^2}{\rho + J_P k^2}}$$

$$v_s(k) = \sqrt{\frac{c_S + a_S k^2}{\rho + J_S k^2}} \qquad v_s(k) = \sqrt{\frac{c_S + (a_S + a_D)k^2}{\rho + J_S k^2}}$$

Hexagonal honeycomb in 2D plane strain

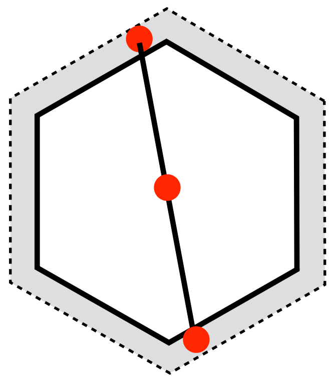

Six rotational symmetries

Six mirror planes

A center of symmetry

$$\begin{pmatrix} \underline{p} \\ \underset{\sim}{q} \\ \underset{\sim}{\sigma} \\ \underset{\approx}{\tau} \end{pmatrix} = \begin{pmatrix} \rho \underset{\sim}{I} & \underset{\simeq}{K} & 0 & 0 \\ \underset{\simeq}{K}^T & \underset{\approx}{J} & 0 & 0 \\ 0 & 0 & \underset{\approx}{C} & \underset{\simeq}{M} \\ 0 & 0 & \underset{\simeq}{M}^T & \underset{\approx}{A} \end{pmatrix} \begin{pmatrix} \underline{v} \\ \nabla \underset{\sim}{v} \\ \underset{\sim}{\varepsilon} \\ \underset{\simeq}{\eta} \end{pmatrix}$$

The generalised Christoffel equation for the directions $\theta = 0°$ and $\theta = 30°$ gives the following phase velocities

$\theta = 0°$

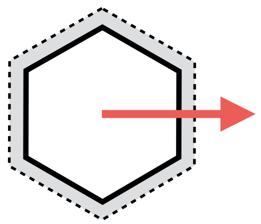

$\theta = 30°$

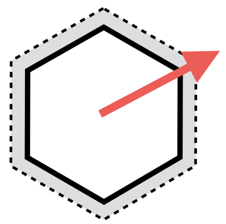

$$v_p(k) = \sqrt{\frac{c_P + (a_P + a_D)k^2}{\rho + J_P k^2}}$$

$$v_p(k) = \sqrt{\frac{c_P + a_P k^2}{\rho + J_P k^2}}$$

$$v_s(k) = \sqrt{\frac{c_S + a_S k^2}{\rho + J_S k^2}}$$

$$v_s(k) = \sqrt{\frac{c_S + (a_S + a_D)k^2}{\rho + J_S k^2}}$$

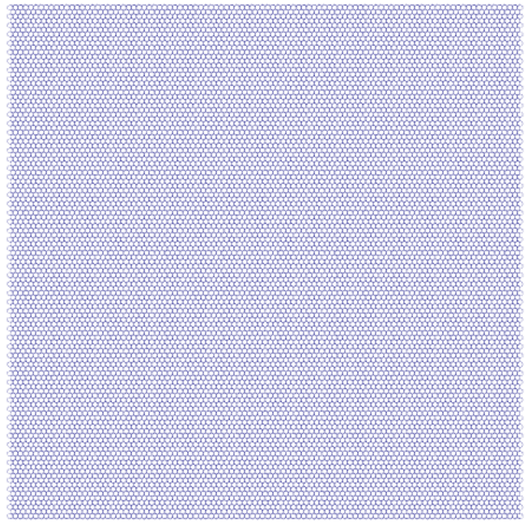

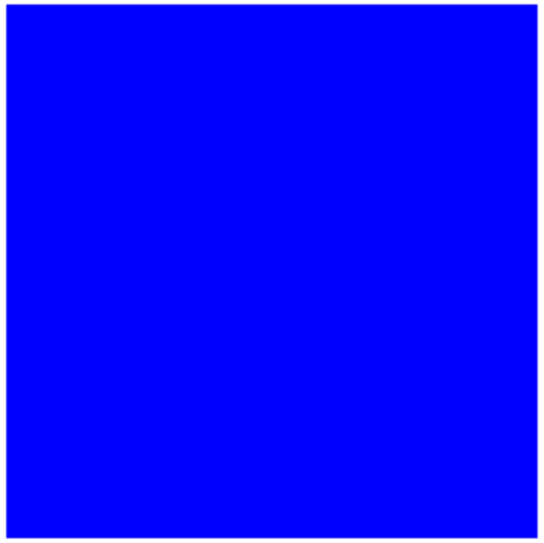

Phase velocities and polarisations

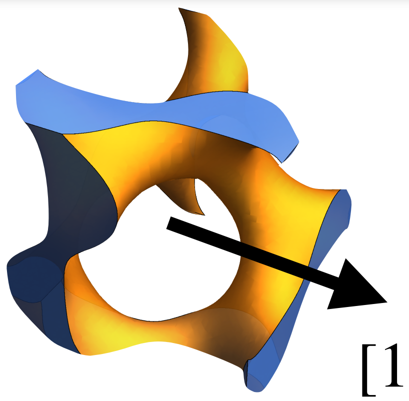

[100]

$$
\begin{pmatrix} \underline{p} \\ \underset{\sim}{q} \\ \underset{\sim}{\sigma} \\ \underset{\simeq}{\tau} \end{pmatrix}
=
\begin{pmatrix}
\rho \underset{\sim}{I} & \underset{\simeq}{K} & 0 & 0 \\
\underset{\simeq}{K}^T & \underset{\approx}{J} & 0 & 0 \\
0 & 0 & \underset{\approx}{C} & \underset{\approxeq}{M} \\
0 & 0 & \underset{\approxeq}{M}^T & \underset{\underset{\sim}{\approx}}{A}
\end{pmatrix}
\begin{pmatrix} \underline{v} \\ \underset{\sim}{\nabla v} \\ \underset{\sim}{\varepsilon} \\ \underset{\simeq}{\eta} \end{pmatrix}
$$

Phase velocities and polarisations

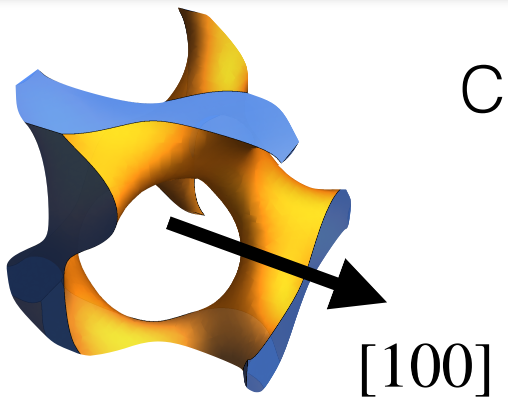

Cubic symmetry

$$\begin{pmatrix} \underline{p} \\ \underset{\sim}{q} \\ \underset{\sim}{\sigma} \\ \underset{\simeq}{\tau} \end{pmatrix} = \begin{pmatrix} \rho \underset{\sim}{I} & \underset{\simeq}{K} & 0 & 0 \\ \underset{\simeq}{K}^T & \underset{\approx}{J} & 0 & 0 \\ 0 & 0 & \underset{\approx}{C} & \underset{\approx}{M} \\ 0 & 0 & \underset{\approx}{M}^T & \underset{\approx}{A} \end{pmatrix} \begin{pmatrix} \underline{v} \\ \underset{\sim}{\nabla v} \\ \underset{\sim}{\varepsilon} \\ \underset{\simeq}{\eta} \end{pmatrix}$$

Phase velocities and polarisations

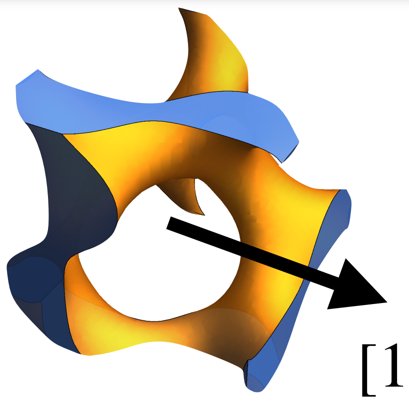

[100]

Cubic symmetry

Chiral

(No center of symmetry)

$$\begin{pmatrix} \underline{p} \\ \underset{\sim}{q} \\ \underset{\sim}{\sigma} \\ \underset{\simeq}{\tau} \end{pmatrix} = \begin{pmatrix} \rho \underset{\sim}{I} & \underset{\simeq}{K} & 0 & 0 \\ \underset{\simeq}{K}^T & \underset{\approx}{J} & 0 & 0 \\ 0 & 0 & \underset{\approx}{C} & \underset{\approxeq}{M} \\ 0 & 0 & \underset{\approxeq}{M}^T & \underset{\approx\approx}{A} \end{pmatrix} \begin{pmatrix} \underline{v} \\ \nabla \underset{\sim}{v} \\ \underset{\sim}{\varepsilon} \\ \underset{\simeq}{\eta} \end{pmatrix}$$

Phase velocities and polarisations

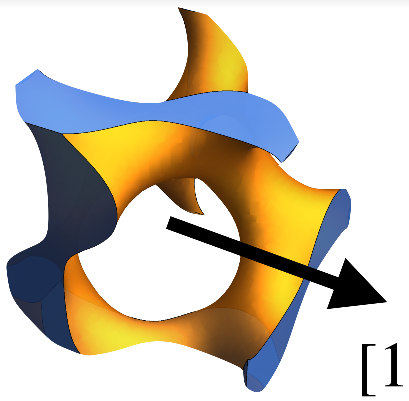

Cubic symmetry

Chiral

(No center of symmetry)

$$\begin{pmatrix} \underline{p} \\ \underset{\sim}{q} \\ \underset{\sim}{\sigma} \\ \underset{\approx}{\tau} \end{pmatrix} = \begin{pmatrix} \rho \underset{\sim}{I} & \underset{\approx}{K} & 0 & 0 \\ \underset{\approx}{K}^T & \underset{\approx}{J} & 0 & 0 \\ 0 & 0 & \underset{\approx}{C} & \underset{\approx}{M} \\ 0 & 0 & \underset{\approx}{M}^T & \underset{\approx}{A} \end{pmatrix} \begin{pmatrix} \underline{v} \\ \nabla \underline{v} \\ \underset{\sim}{\varepsilon} \\ \underset{\approx}{\eta} \end{pmatrix}$$

The generalised Christoffel equation for the direction $\underline{n} = [010]$ gives the following phase velocities

$$v_1 = \sqrt{\frac{c_{44} - km_1 + k^2 a_{S_1}}{\rho - kK + k^2 j_{S_1}}} \qquad v_2 = \sqrt{\frac{c_{44} + km_1 + k^2 a_{S_1}}{\rho + kK + k^2 j_{S_1}}} \qquad v_3 = \sqrt{\frac{c_{11} + k^2 a_P}{\rho + k^2 j_P}}$$

Phase velocities and polarisations

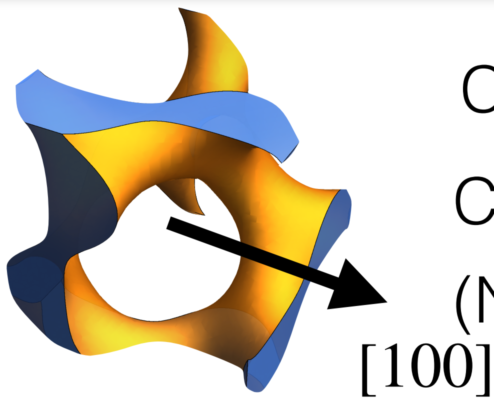

Cubic symmetry

Chiral

(No center of symmetry)

$$\begin{pmatrix} \underline{p} \\ \underset{\sim}{q} \\ \underset{\sim}{\sigma} \\ \underset{\approx}{\tau} \end{pmatrix} = \begin{pmatrix} \rho \underset{\sim}{I} & \underset{\approx}{K} & 0 & 0 \\ \underset{\approx}{K}^T & \underset{\approx}{J} & 0 & 0 \\ 0 & 0 & \underset{\approx}{C} & \underset{\approx}{M} \\ 0 & 0 & \underset{\approx}{M}^T & \underset{\approx}{A} \end{pmatrix} \begin{pmatrix} \underline{v} \\ \nabla \underset{\sim}{v} \\ \underset{\sim}{\varepsilon} \\ \underset{\approx}{\eta} \end{pmatrix}$$

The generalised Christoffel equation for the direction $\underline{n} = [010]$ gives the following phase velocities

$$v_1 = \sqrt{\frac{c_{44} - km_1 + k^2 a_{S_1}}{\rho - kK + k^2 j_{S_1}}} \qquad v_2 = \sqrt{\frac{c_{44} + km_1 + k^2 a_{S_1}}{\rho + kK + k^2 j_{S_1}}} \qquad v_3 = \sqrt{\frac{c_{11} + k^2 a_P}{\rho + k^2 j_P}}$$

Phase velocities and polarisations

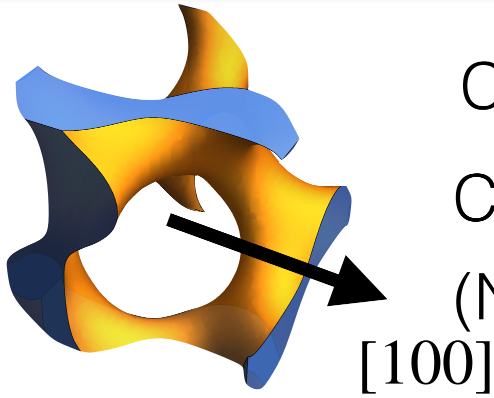

Cubic symmetry

Chiral

(No center of symmetry)

$$\begin{pmatrix} \underline{p} \\ \underset{\sim}{q} \\ \underset{\sim}{\sigma} \\ \underset{\approx}{\tau} \end{pmatrix} = \begin{pmatrix} \rho \underset{\sim}{I} & \underset{\approx}{K} & 0 & 0 \\ \underset{\approx}{K}^T & \underset{\approx}{J} & 0 & 0 \\ 0 & 0 & \underset{\approx}{C} & \underset{\approx}{M} \\ 0 & 0 & \underset{\approx}{M}^T & \underset{\underset{\sim}{\approx}}{A} \end{pmatrix} \begin{pmatrix} \underline{v} \\ \underset{\sim}{\nabla v} \\ \underset{\sim}{\varepsilon} \\ \underset{\approx}{\eta} \end{pmatrix}$$

The generalised Christoffel equation for the direction $\underline{n} = [010]$ gives the following phase velocities

$$v_1 = \sqrt{\frac{c_{44} - km_1 + k^2 a_{S_1}}{\rho - kK + k^2 j_{S_1}}} \qquad v_2 = \sqrt{\frac{c_{44} + km_1 + k^2 a_{S_1}}{\rho + kK + k^2 j_{S_1}}} \qquad v_3 = \sqrt{\frac{c_{11} + k^2 a_P}{\rho + k^2 j_P}}$$

Phase velocities and polarisations

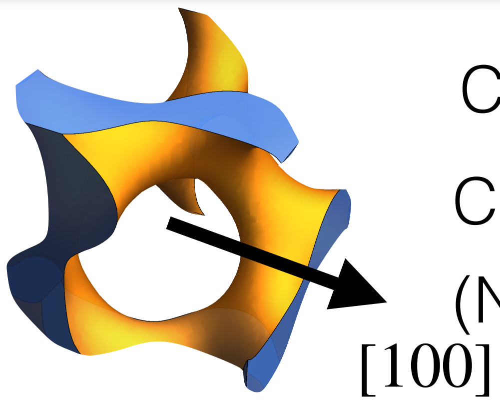

Cubic symmetry

Chiral

(No center of symmetry)

$$\begin{pmatrix} \underline{p} \\ \underset{\sim}{q} \\ \underset{\sim}{\sigma} \\ \underset{\approx}{\tau} \end{pmatrix} = \begin{pmatrix} \rho \underset{\sim}{I} & \underset{\approx}{K} & 0 & 0 \\ \underset{\approx}{K}^T & \underset{\approx}{J} & 0 & 0 \\ 0 & 0 & \underset{\approx}{C} & \underset{\approx}{M} \\ 0 & 0 & \underset{\approx}{M}^T & \underset{\approx}{A} \end{pmatrix} \begin{pmatrix} \underline{v} \\ \underset{\sim}{\nabla v} \\ \underset{\sim}{\varepsilon} \\ \underset{\approx}{\eta} \end{pmatrix}$$

The generalised Christoffel equation for the direction $\underline{n} = [010]$ gives the following phase velocities

$$v_1 = \sqrt{\frac{c_{44} - km_1 + k^2 a_{S_1}}{\rho - kK + k^2 j_{S_1}}} \qquad v_2 = \sqrt{\frac{c_{44} + km_1 + k^2 a_{S_1}}{\rho + kK + k^2 j_{S_1}}} \qquad v_3 = \sqrt{\frac{c_{11} + k^2 a_P}{\rho + k^2 j_P}}$$

Phase velocities and polarisations

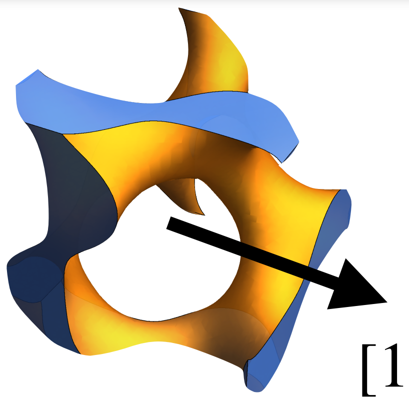

Cubic symmetry

Chiral

(No center of symmetry)

$$\begin{pmatrix} \underline{p} \\ \underset{\sim}{q} \\ \underset{\sim}{\sigma} \\ \underset{\approx}{\tau} \end{pmatrix} = \begin{pmatrix} \rho \underset{\sim}{I} & \underset{\approx}{K} & 0 & 0 \\ \underset{\approx}{K}^T & \underset{\approx}{J} & 0 & 0 \\ 0 & 0 & \underset{\approx}{C} & \underset{\approx}{M} \\ 0 & 0 & \underset{\approx}{M}^T & \underset{\approx}{A} \end{pmatrix} \begin{pmatrix} \underline{v} \\ \nabla \underset{\sim}{v} \\ \underset{\sim}{\varepsilon} \\ \underset{\approx}{\eta} \end{pmatrix}$$

The generalised Christoffel equation for the direction $\underline{n} = [010]$ gives the following phase velocities

$$v_1 = \sqrt{\frac{c_{44} - km_1 + k^2 a_{S_1}}{\rho - kK + k^2 j_{S_1}}} \qquad v_2 = \sqrt{\frac{c_{44} + km_1 + k^2 a_{S_1}}{\rho + kK + k^2 j_{S_1}}} \qquad v_3 = \sqrt{\frac{c_{11} + k^2 a_P}{\rho + k^2 j_P}}$$

and complex polarisations

$\underline{u}_1 = (0, -i, 1)$ $\qquad$ $\underline{u}_2 = (0, i, 1)$ $\qquad$ $\underline{u}_3 = (0,0,1)$

Circular LH $\qquad$ Circular RH $\qquad$ Linear

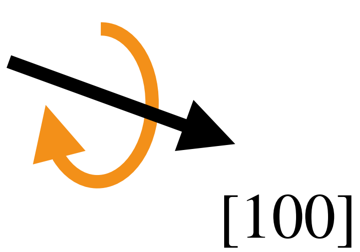

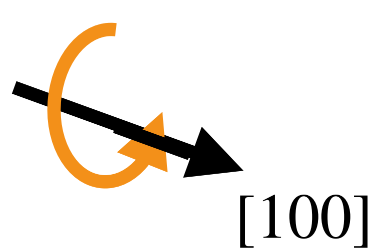

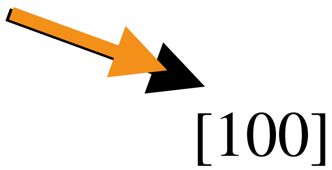

$$\underline{u}_1 \cdot \underline{u}_1 = 0 \qquad \left[\underline{u}_2^R \ \underline{u}_2^I \ \underline{n}\right] > 0$$

$$\underline{u}_2 \cdot \underline{u}_2 = 0 \qquad \left[\underline{u}_2^R \ \underline{u}_2^I \ \underline{n}\right] < 0$$

$$\underline{u}_3^R \times \underline{u}_3^I = \underline{0}$$

Conclusions and perspectives

Main results

- Generalised continua are an effective tool to study wave propagation in architectured material
- Results from metamaterials can be of use in biomechanics

Perspectives for biomechanical metamaterials

- Optimisation of ultrasonic properties (tailored ultrasonic signature)
- Enhanced osteointegration monitoring
- Real time quality assessment of the microstructure (phononic properties)

Things to do next

- Experimental validation (in progress)
- Reliable procedure for the estimation of the coefficients (based on guided propagation)

References

[1] N. Auffray, J. Dirrenberger, and G. Rosi, "A complete description of bi-dimensional anisotropic strain-gradient elasticity," Int. J. Solids. Struct., vol. 69, pp. 195–206, 2015.

[2] G. Rosi and N. Auffray, "Anisotropic and dispersive wave propagation within strain-gradient framework," Wave Motion, vol. 63, pp. 120–134, 2016.

[3] G. Rosi, L. Placidi, and N. Auffray, "On the validity range of strain-gradient elasticity: A mixed static-dynamic identification procedure," Eur. J. Mech. A-Solids, vol. 69, pp. 179–191, 2018.

[4] G. Rosi and N. Auffray, "Continuum modelling of frequency dependent acoustic beam focusing and steering in hexagonal lattices", Eur. J. Mech. A-Solids, 2019

[5] G. Rosi, N. Auffray, C. Combescure (2020). On the failure of classic elasticity in predicting elastic wave propagation in gyroid lattices for very long wavelengths. Symmetry

Polarisation of waves

Gyroid architectures can sustain circular polarisation.

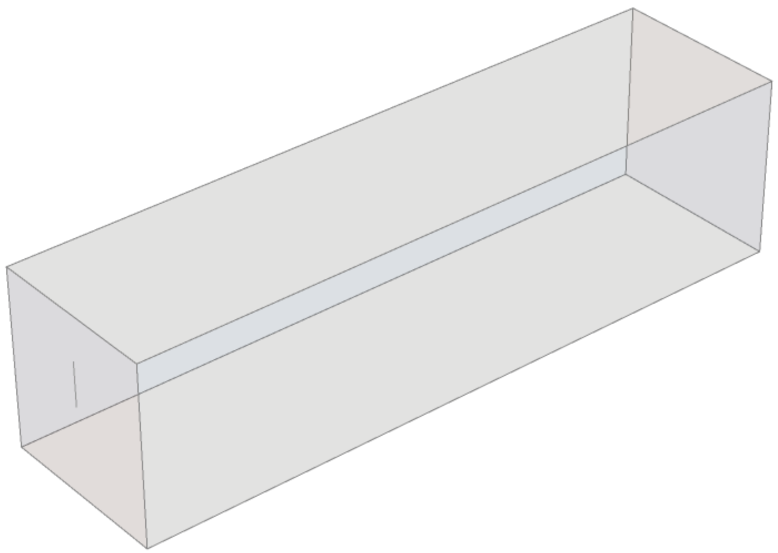

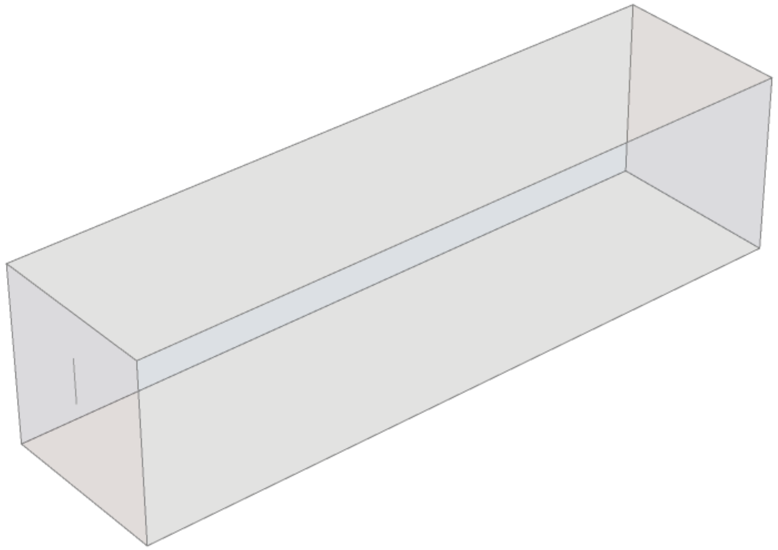

Circularly polarised waves does not propagate at the same speed

Rosi, G., Auffray, N., Combescure, C. (2020). On the failure of classic elasticity in predicting elastic wave propagation in gyroid lattices for very long wavelengths. Symmetry

Polarisation of waves

Gyroid architectures can sustain circular polarisation.

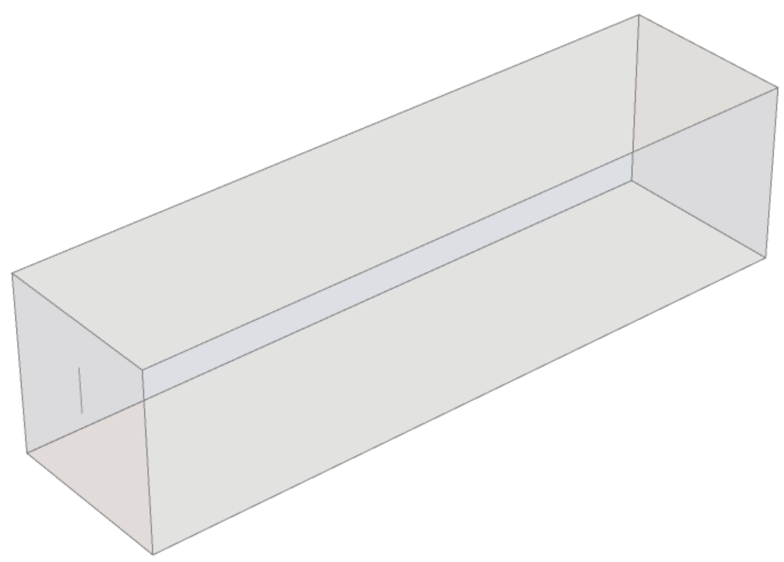

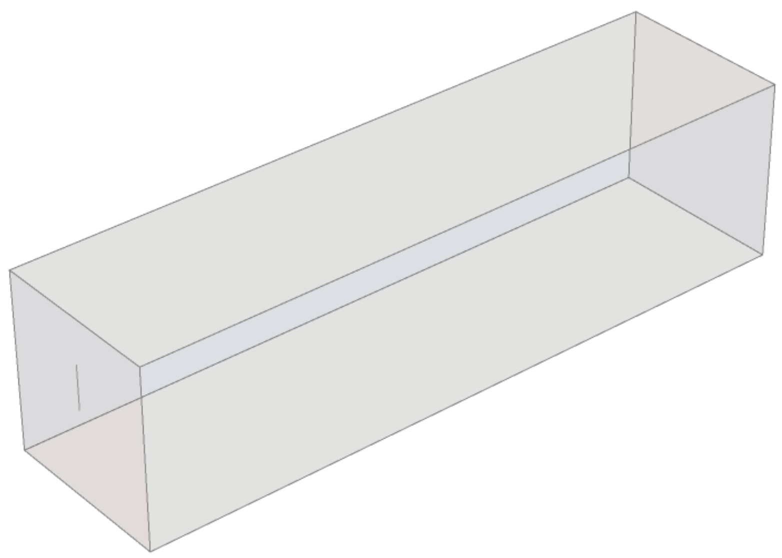

Circularly polarised waves does not propagate at the same speed

Rosi, G., Auffray, N., Combescure, C. (2020). On the failure of classic elasticity in predicting elastic wave propagation in gyroid lattices for very long wavelengths. Symmetry

Polarisation of waves

Gyroid architectures can sustain circular polarisation.

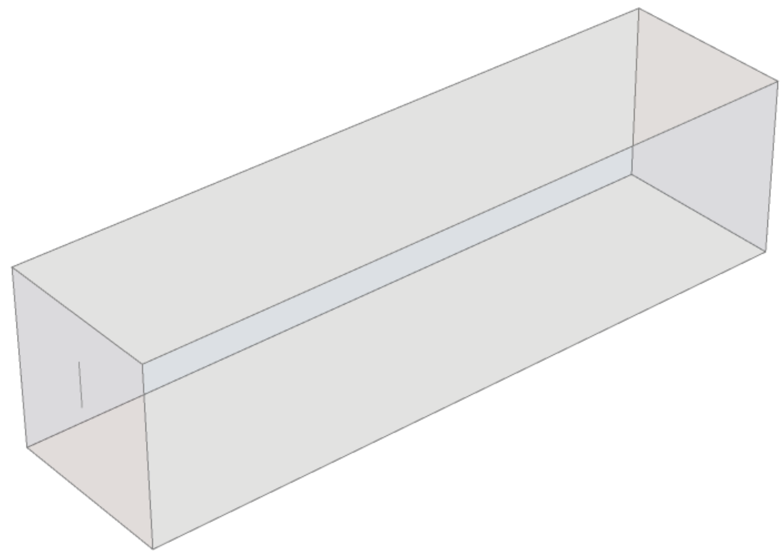

+

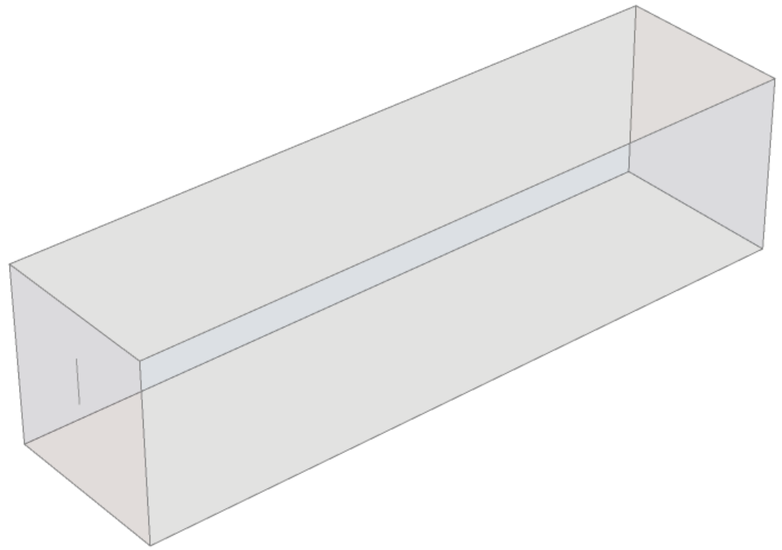

Circularly polarised waves does not propagate at the same speed

Rosi, G., Auffray, N., Combescure, C. (2020). On the failure of classic elasticity in predicting elastic wave propagation in gyroid lattices for very long wavelengths. Symmetry

Polarisation of waves

Gyroid architectures can sustain circular polarisation.

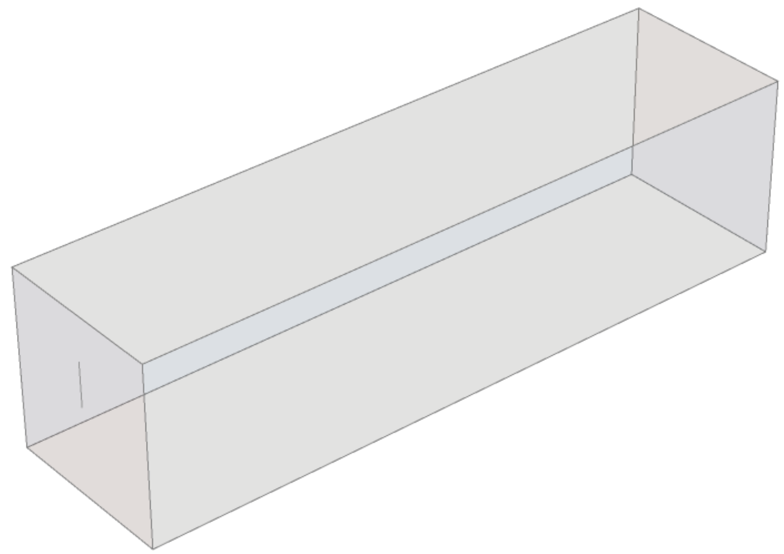

+

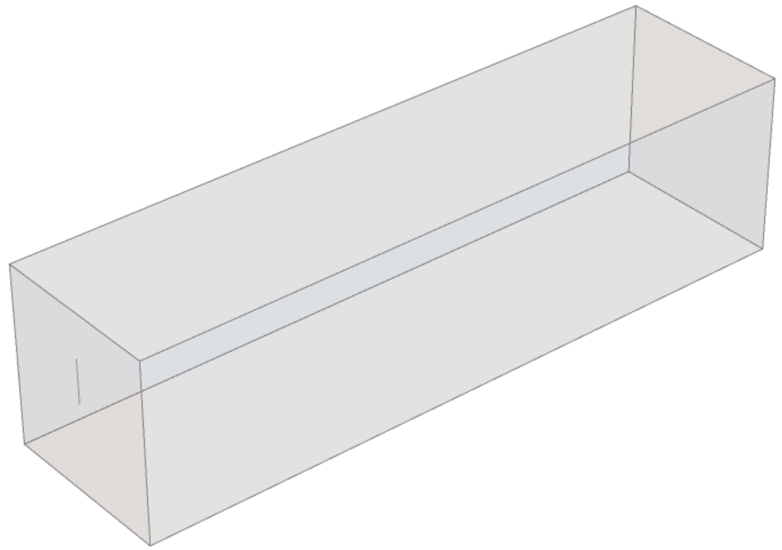

Circularly polarised waves does not propagate at the same speed

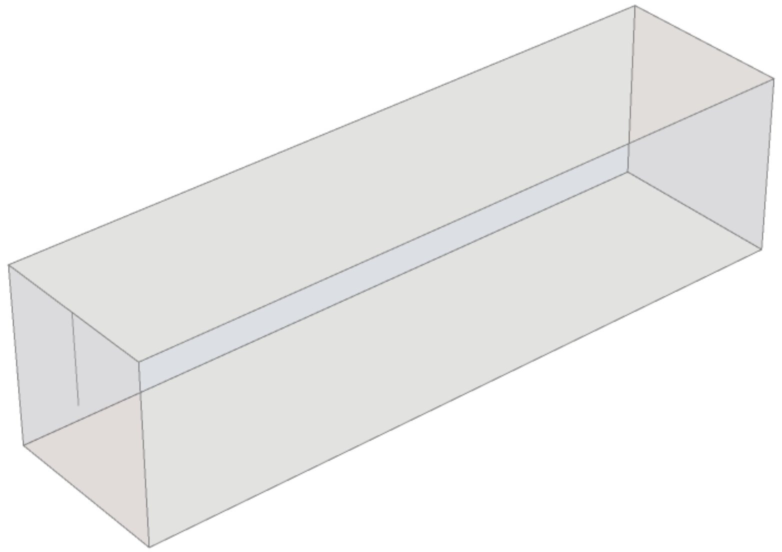

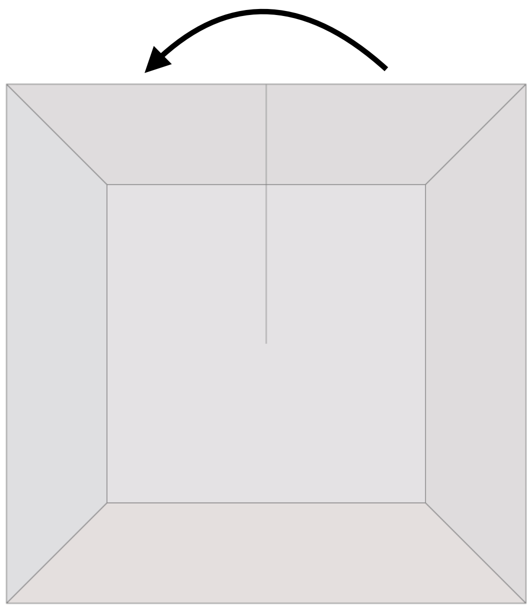

Rosi, G., Auffray, N., Combescure, C. (2020). On the failure of classic elasticity in predicting elastic wave propagation in gyroid lattices for very long wavelengths. Symmetry

Some additional motivations from crystallography

Neumann's principle (Curie laws)

"if a **crystal** is **invariant** with respect to certain **symmetry operations**, any of its **physical properties** must also be **invariant** with respect to the **same symmetry operations**"

or otherwise stated

"**the symmetry operations of any physical property of a crystal must include the symmetry operations of the point group of the crystal**"

Some additional motivations from crystallography

Neumann's principle (Curie laws)

"if a **crystal** is **invariant** with respect to certain **symmetry operations**, any of its **physical properties** must also be **invariant** with respect to the **same symmetry operations**"

or otherwise stated

"**the symmetry operations of any physical property of a crystal must include the symmetry operations of the point group of the crystal**"

Hermann theorem of crystal physics

If we consider a **r-rank** tensor with reference to a material having a **N-fold axis of symmetry**, and **r<N**, then this tensor property affectively conforms to an **infinitely-fold symmetry axis parallel to the N-fold axis**.

Hermann theorem provides a sufficient condition for transverse anisotropy